Autogenous Self-Healing of Concrete: Experimental Design and Test Methods – A Review

Daniel Lahmann, Carola Edvardsen and Sylvia Kessler*

D. Lahmann , Prof. S. Kessler
Institute of Engineering Materials and Building Preservation Helmut-Schmidt-University/University of the Federal Armed Forces Hamburg, Charlie Mills-Straße 2, 22159 Hamburg, Germany
E-mail: lahmannd@hsu-hh.de

Dr. C. Edvardsen
COWI Technical Director/Lead Durability Specialist Tunnels and Underground Infrastructure, Parallelvej 2, 2800 Kongens Lyngby, Denmark

Keywords: autogenous self-healing, concrete, influencing factors, experimental designs

Cracks in concrete structures can serve as pathways for aggressive chemical substances that can lead to a progressive deterioration of the cement stone as well as of the reinforcement, affecting the load capacity, service life and useability of concrete structures. However, concrete and reinforced concrete exhibit an intrinsic ability to heal cracks, defined as autogenous self-healing. This effect includes the precipitation of calcium carbonate in the presence of water and CO_2 and is accompanied by continued hydration, swelling and mechanical blocking of the crack pathway. Experiments led to the inclusion of crack sealing by autogenous self-healing in Eurocode 1992-3 for water retaining concrete structures. However, despite code restrictions, autogenous self-healing of concrete shows limited effectiveness in practice. This indicates the need for further research to provide engineers with reliable design rules. Therefore, this study aims for giving a broad literature review on the state-of-the-art knowledge on autogenous self-healing, the boundary conditions, consensus and controversy of processes and factors influencing the efficiency of autogenous self-healing. Regarding the transferability of laboratory results to real concrete constructions, materials, crack initiation techniques, experimental concepts and methods for assessing the effectiveness of autogenous self-healing are discussed and recommendations for future experiments are set.

1 Introduction

Modern design and construction are highly dependent on the composite material concrete, which is made of aggregates, cement, water, admixtures and additives. A combination of desirable properties such as a high compressive strength, a broad availability of its raw materials and a superior cost efficiency make concrete the most widely used construction material in the

world [1–3]. However, due to its low tensile strength the formation of cracks from micro to macro scale due to load and load independent deformation caused by e.g., shrinkage, is unavoidable. Furthermore, it is necessary to reinforce concrete for many applications. Typically, inside concrete components steel bars bring the required tensile strength into the structure. This material is commonly known as reinforced concrete. The high *pH* of cement phases and pore solutions around 13.5 protects the rebars from corroding by the formation of a passive layer on the surface of the steel [3–5]. Thus, reinforced concrete could be considered a durable composite material. However, cracks can act as pathways for aggressive chemical substances that can lead to a progressive deterioration of the cement stone as well as of the rebars, affecting the load capacity, service life and useability of concrete structures [6,7].

Concrete and reinforced concrete exhibit an intrinsic ability to heal cracks, defined by RILEM technical committee as "autogenous self-healing" [8]. This effect includes the precipitation of calcium carbonate in the presence of water and CO_2 and is accompanied by continued hydration, swelling and mechanical blocking of the crack pathway. Autogenous self-healing has been investigated by many researchers since the 1980s [9–13] as a possibility to restore load capacity, durability and useability of concrete structures. These experiments led to the formulation of Eurocode 1992-3 [14] that regulates the boundary conditions, crack widths and hydraulic gradients under which autogenous self-healing is likely to occur. For reinforced concrete structures that have an increased demand on durability, the maximum crack width w_{max} is limited to 300 µm. For water retaining concrete structures w_{max} is further limited to 200 µm with respect to the ratio of water head to wall thickness. However, in practice it is observed that cracks in accordance with the restriction do not heal [15]. Problems might be that laboratory results have not been verified at real concrete structures as of today, or even worse, cracks do not heal because the boundary conditions are neglected on-site. Furthermore, as proof of the appropriate application of the restrictions the calculated crack width w_k is set equal to w_{max} according to DIN 1045-1:2008 , which can have severe consequences [15,16]. The scattering of crack widths due to crack geometry, temperature, loading, etc. is neglected and, as a matter of fact, it is accepted that for w_k of 200 µm 20 % of the measured crack widths can be greater than the actual restriction of 200 µm. Moreover, there still is a general lack of a comprehensive understanding of the relevant processes of autogenous self-healing.

Therefore, this study aims at reviewing and discussing the scientific consensus and controversy about parameters influencing autogenous self-healing, materials, experimental designs and methods applied to assess the healing efficiency of cracked concrete. To guide the reader through this document self-explanatory icons were designed that represent certain aspects

within the workflow of autogenous self-healing experiments (**Figure 1**). These icons are repeated in the corresponding chapters for the reader`s convenience. In chapter 2 (icon: books) the process theory of autogenous self-healing is covered. In chapter 3 (icon: hammer and trowel) materials and crack initiation techniques are discussed and recommendations for future experiments that aim at the reliable transfer of laboratory results to real concrete constructions are given. In chapter 4 (icon: plaster), different exposure conditions that can be applied to initiate autogenous self-healing are covered. Followed by an overview of the possibilities and limitations of analytical methods that can be applied to assess the efficiency of autogenous self-healing in chapter 5 (icon: magnifying glass). This contributes to a comprehensive understanding of the relevant processes of autogenous self-healing, how they can be examined and quantified and where further research should be carried out in the future.

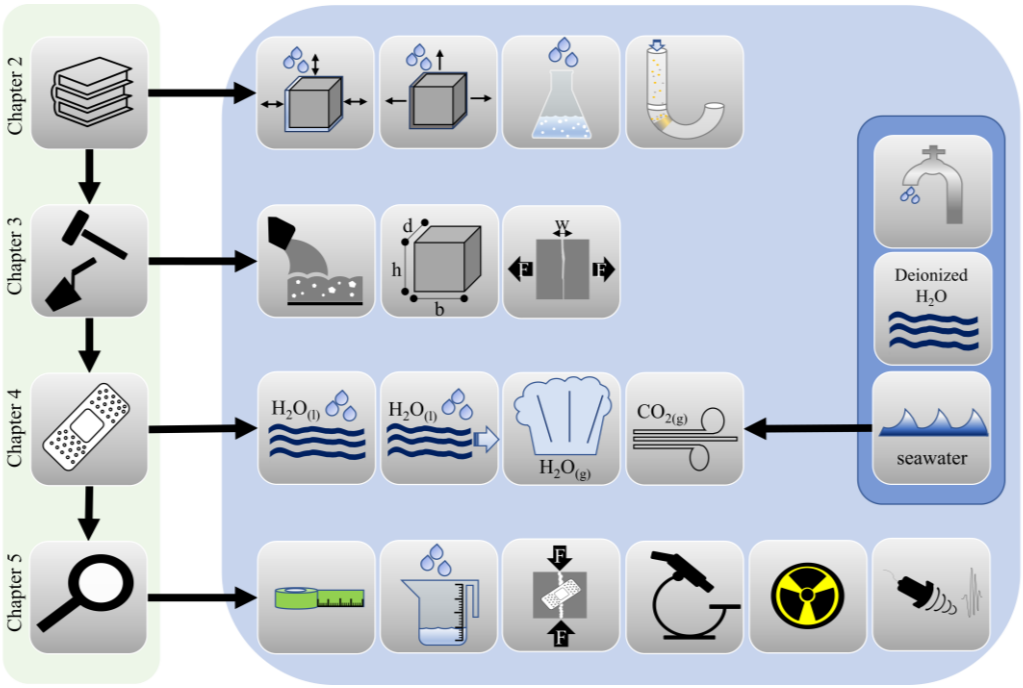

Figure 1. Schematic overview of the workflow of autogenous self-healing experiments.

2 Processes of Autogenous Self-healing

Autogenous self-healing can be subdivided in three main causes, (1) a physical cause: swelling of concrete, (2) chemical causes: continued hydration of unhydrated cement phases and formation of calcium carbonate, and (3) mechanical causes: clogging of the flow path due to fine particles in the water and loose concrete particles [8,11] (**Figure 2**). Concerning the mechanical causes, flow of liquid water is required whereas chemical causes require only the

presence of liquid water. The swelling of concrete is also possible in highly moist environments. It is widely accepted that in the presence of liquid water that is in equilibrium with a CO_2 rich atmosphere such as air, the formation of calcium carbonate is the predominant process of autogenous self-healing [10,11,17–20]. A detailed discussion of the causes is given below (comp. 2.1 to 2.4). Maximum crack widths that can be healed by autogenous self-healing can be found in the range of 5 to 300 µm [21]. Differences can be assigned to different experimental setups and specimen compositions, the number of tested specimens and applied assessment methods.

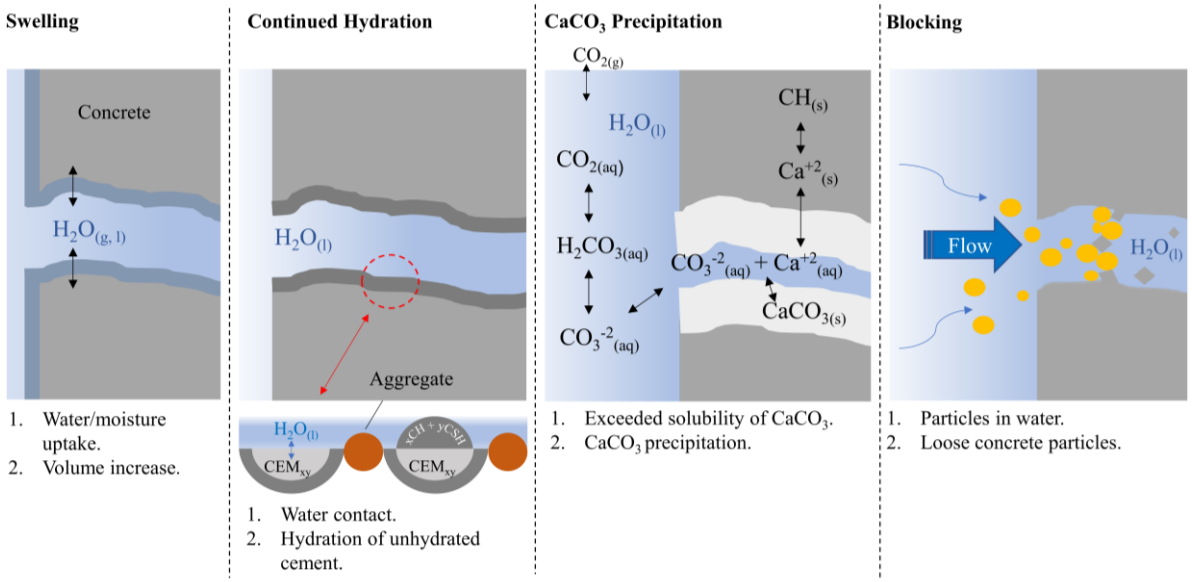

Figure 2. Schematic overview of possible causes of autogenous self-healing.

2.1. Swelling

Swelling of concrete is a slow and theoretically partly reversible process caused by water adsorption of the cement stone [10,11]. Thus, a crack sealed due to swelling can become leaky again in a dry period and close again in the presence of water or sufficient humidity. In practice, however, it is difficult to determine the isolated effect of swelling of concrete without measuring superimposed processes such as autogenous shrinkage, excessive calcite precipitation or continued hydration. For instance, Meichsner [10] measured the volume flow through a separating crack that was healed under flow conditions and then exposed to a dry environment for at least one week. As expected, the crack became leaky after the dry period. Accordingly, the experiment was repeated four times whereas with every repetition the increase of volume flow became less pronounced. Therefore, swelling is not a completely reversible process. However, it must be addressed that superimposed effects cannot be excluded for this

experimental setup. According to Edvardsen [11] swelling is of little importance for crack closing of cracks wider ≥ 100 µm. The author gives a crack width reduction of 6 µm which was obtained through a sample calculation assuming a penetration depth of 30 mm and a maximum swelling of 0.1 mm*m^{-1}. This contradicts with results from Meichsner [10] who measured swelling with 0.3 mm*m^{-1} on samples that were submerged in water. Based on this and an assumed penetration depth of approx. 42 mm the latter author gives a theoretical crack width reduction of 25 µm. Therefore, differences in the sample calculations of Meichsner and Edvardsen can be explained by the lack of reliable data on the penetration depth and assumed degree of swelling. Roig-Flores et al. [22] found out that cracks can close by up to 8 % when exposed to 95 % relative humidity (**RH**) and 20 °C. However, when the environment was sufficiently dry (RH ~ 45 %) the crack width increased by up to 46 % due to drying shrinkage. The initial crack widths are given with w < 300 µm but were not further limited. This makes it difficult to compare the measured value with Meichsners and Edvardsens theoretical values. Interestingly, however, experiments in humidity chambers could provide a possibility to quantify the effect of swelling without the superimposed effects of continued hydration, calcite precipitation or clogging of the flow path. However, it must be addressed that moisture and liquid water, water pressure, temperature and physical properties of the samples could result in different values for swelling. Finally, it can be concluded that for cracks restricted by Eurocode 1992-3 [14] a maximum of 6 % to 25 % of the initial crack width (w ~ 100 µm) could be closed due to swelling. To date, however, there still is a lack of reliable data on swelling with respect to autogenous self-healing.

2.2 Continued Hydration

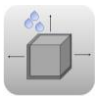

According to *Ritzmann* [23] the hydration depth of cement particles is 5 µm after 28 days of hydration. During longer hydration periods particles up to 10 µm can hydrate completely [24]. The particle sizes of cement range from 0 µm to 100 µm whereas the exact particle size distribution depends on the desired properties of the cement such as for instance early age strength. The average grain size of CEM I/32.5 is in the range of 10 to 20 µm [3]. Therefore, especially with concrete at a young age, unhydrated cement particles are available for continued hydration when the particles are exposed to additional water. Therefore, continued hydration and its effect on autogenous self-healing has been studied [19,20,25–27]. Some studies assign the uncertain effect of autogenous self-healing in practice to an excessive overgrinding of modern cements and suggest an optimized average cement grain size to improve the effect of continued

hydration [19,28]. However, a practical relevance for this suggestion is questionable concerning the impact on concrete properties such as strength. According to *Edvardsen* [11] continued hydration is of minor importance for crack closing as no proof for it could be seen in her experimental study with cracked CEM I/32.5 R, CEM III/A 32.5 N (45 % ground blast furnace slag (**BFS**)) and CEM III/A 32.5 N LH/SR (22 % BFS) concretes subjected to continuous water flow. In case hydration products were washed away or overlooked she also provides an example calculation. Assuming a uniform particle diameter of 50 µm, a volume doubling for complete hydration and a hydration degree of 5 % after three days, a crack width reduction of approx. 6 µm can be calculated for complete hydration. Therefore, the author states that continued hydration and swelling of concrete are in a similar range (comp. 2.1) and only of importance for cracks << 100 µm. However, some studies aimed at isolating the effect of continued hydration, whereas special precautions must be taken to avoid excessive carbonation. Typically, experiments are carried out with deionized water and under a CO_2 free atmosphere [25,29]. *Yuan et al.* [19] found continued hydration for CEM I mortar specimens in the range of 12 to 22 µm after seven days of self-healing in water immersion. The initial crack width was ~ 300 µm and the sample age 28 days. The authors also state, that continued hydration is the main mechanism of healing during the first seven days of healing. Afterwards excessive carbonation is taking over. However, the water chemistry and atmospheric conditions are not clearly stated. Thus, this apparently delayed carbonation could be caused by the kinetics of dissolution of CO_2 in deionized water. *Huang et al.* [26,27] give a value of 30 to 35 % of 10 µm cracks in CEM I cement paste that could be healed by capillary suction of water or $Ca(OH)_2$ solution under a CO_2 free atmosphere after an exposure time of 250h. A higher healing efficiency was achieved for CEM III cement with approx. 60 % of 10 µm cracks healed by capillary suction of $Ca(OH)_2$ solution. Generally healing was more efficient in $Ca(OH)_2$ solution. Interestingly, for both water and $Ca(OH)_2$ solution the hydration is fastest in the first 48h and slows down distinctly afterwards. This could affect rapid flow reduction in permeability experiments (comp. 4.3). Yet, differences between the authors could be assigned to the variable experimental approaches and materials. However, the scattering of ~ 3 to 22 µm of possible crack width reduction by continued hydration is severe and should be investigated in further research. An influence of the initial crack width seems possible. Furthermore, it is desirable to study crack width reduction through continued hydration of specimens that were subjected to a permeation test. Respectively, the adhesion force of hydration products and critical water pressure that can be withstand could be determined. To obtain results that are transferable to real structures, concrete samples instead of mortar or paste should be used.

Huang et al. [26,27] characterized the phases that formed due to continued hydration chemically and mineralogically (see above for experimental conditions). The authors subdivided the hydration products into gel-like and crystal-like hydration products. For CEM I cement, the phases formed by continued hydration amount to approx. 78 % to crystal-like $Ca(OH)_2$ (**CH**) and 5 % $CaCO_3$ and 17 % to gel-like calcium-silicate-hydrate (**CSH**) as determined by x-ray diffraction (**XRD**) and thermogravimetric analysis/differential thermal analysis (**TG/DTA**). For CEM III cement the phase content is different. Respectively, approx. 6 % CH, 7.5 % Mono ($Ca_4Al_2(CO_3)(OH)_{12}*5H_2O$) and Hemi-Carboaluminate ($Ca_4Al_2(CO_3)_{0.5}(OH)_{13}*5.5H_2O$), 9.5 % Ettringite ($Ca_6Al_2(SO_4)_3(OH)_{12}*26\ H_2O$), 20 % $CaCO_3$ and 57 % CSH were determined by XRD and TG/DTA. A general depletion of Si^{4+} in the hydration products compared to the cement stone matrix was measured by environmental scanning electron microscopy (**ESEM**). This was attributed to the slower diffusion of Si^{4+} with respect to Ca^{2+}. Detected $CaCO_3$ and Mono- and Hemi-Carboaluminate was assigned to the successive reaction of CH with atmospheric CO_2 after the experiment was terminated. Concerning the different phase composition that is formed by continued hydration, it can be assumed that the cement type impacts the extend of carbonation secondarily through the CH content in the hydration margin, since CH is the main source of Ca^{2+} ions which are required for carbonation [11]. This effect could be accompanied by a generally lower content of CH in cements incorporating pozzolanic or latent hydraulic replacements such as fly ash or ground blast furnace slag (comp. 2.3). Yet, the understanding of the impact of continued hydration on carbonation and the dove-tailing of these two healing processes is little. For instance, it remains questionable whether primary carbonation of CH and unhydrated cement clinker phases in the cement stone matrix exposed at the crack wall takes places before any continued hydration.

Since cements incorporating pozzolanic or latent hydraulic supplementary cementitious materials show a slower hydration process, the potential for enhanced continued hydration was widely discussed in the literature [25,30–35]. According to *Van Tittelboom et al.* [25] best self-healing results can be obtained by cements incorporating blast furnace slag or fly ash replacement and thus showed a lower hydration degree at the testing age of 55 days compared to ordinary Portland cement. Respectively, the latter authors found that increasing the water/cement (***W/C***) ratio had the opposite effect. The results base on the assumption that only continued hydration is responsible for the flow reduction in the permeability experiments that were carried out with cracked mortar specimens and deionized water in a CO_2 free environment. However, it must be addressed that mineralogical and chemical proof was not given in the study and the possibility of physical clogging of the flow path was not discussed. Moreover, the

results are in contradiction with findings of *Maes* [20] who states that the extend of continued hydration is independent from the used cement type. The author refers to experiments with CEM I and CEM III mortar specimens that were subjected to healing in deionized water immersion at the age of 24 days. The healing was then measured in terms of crack width measurements. Thus, differences between the authors could also be assigned to the age of the specimens and the subjective crack width measurement technique. Nevertheless, the supportive effect on continued hydration through the partial replacement of Portland cement with fly ash was also found in other studies [32–36]. *Zhou et al.* [34] even recommend the incorporation of 40 % fly ash in cement to obtain best self-healing results. However, these studies have in common that the effect of continued hydration was investigated by compression strength, porosity, hydration degree or Cl^- diffusion coefficient measurements. Thus, the results are based on measurements of physical properties that are not relevant for the flow reduction of thru cracked concrete. Respectively, *Termkhajornkit et al.* [33] states that his results are only applicable to the healing of micro-cracked cement paste and does e.g. account for the regain of strength [34,37] whereas the ability of continued hydration to heal wider cracks is questionable. Regardless the controversial results concerning continued hydration it can be concluded that hydration reactions are possibly of major importance for healing cracks with $w << 100$ µm. With respect to a comprehensive numerical modelling of autogenous self-healing further research is required to improve the understanding of continued hydration, dove-tailing of chemical processes and the impact on carbonation.

2.3 Calcium-Carbonate Formation

It is widely accepted that calcium carbonate precipitation is the main mechanism of autogenous self-healing when cracked concrete is healed in liquid fresh water with a $pH \approx 7$ in equilibrium to a CO_2 rich atmosphere such as air [10,11,17–20]. Ca^{2+} ions from the concrete react with carbonate species in the water and precipitate as calcite as soon as the solubility is exceeded. *Edvardsen* [11] showed that under the aforementioned conditions calcite is the thermodynamically stable structure of $CaCO_3$ and can close cracks up to 200 µm width completely when specimens are subjected to water flow for a few days to several weeks. It is also the only cause of autogenous self-healing that could be proven by the authors chemical and mineralogical analysis of healing products after the experiments were terminated. *Edvardsen* further determined that the extent of flow reduction is independent from the cement type,

additives increasing the Ca^{2+} content and the concentration of carbonate species in the permeating water. This is in accordance with results from *Meichsner* [10]. Measurements of the chemical composition of the permeated water further showed that there is always an excess of HCO_3^-, CO_3^{2-} and Ca^{2+} ions available for calcite formation.

However, it was observed in other studies that the partial replacement of Portland cement by ground blast furnace slag or fly ash reduces the amount of formed calcite [17,25,38]. This was assigned to a limited availability of Ca^{2+} ions that mainly originate from portlandite (comp. 2.2). On the other hand, *Suleiman et al.* [39] showed that cements with added limestone powder exhibit a higher maximum healable crack width by calcite precipitation compared to Portland cement references. Moreover, the authors showed that for limestone cements, the measured Ca^{2+} concentration in the deionized water of the immersion tests was higher than for Portland cement. Thus, limestone additives could promote calcium carbonate formation. However, the latter results contradict the finding of *Edvardsen* and *Meichsner*. Furthermore, these studies are based on mortar or concrete specimens that were submerged in water for healing while the extend of healing was measured by surface crack width measurements. In contrast, *Meichsner* and *Edvardsen* conducted permeation experiments. Thus, differences could be assigned to the experimental approach and assessment technique of autogenous self-healing. However, it is desirable that *Edvardsens* and *Meichsners* results are verified on modern cements which typically have a low Portland cement content and can contain different cementitious supplementary materials.

Generally, calcite precipitation or dissolution depends on the *pH* value, temperature and the partial pressure of CO_2 (**pCO_2**) [3,11]. Regarding the equilibrium of the $CaCO_3$-CO_2-H_2O system the solubility of calcite increases with lowering of the *pH* value, decreasing temperature and increasing pCO_2. Thus, in practice autogenous self-healing approaches cannot be applied when concrete attacking water with a *pH* value < 5.5 or > 40 mg*l^{-1} CO_2 is present as recommended by the Germen board for reinforced concrete (DAfStb) [40]. However, assuming the concentration of Ca^{2+} ions in the crack to be constant (thus equal to one in the solubility calculation) one can calculate a critical *pH* ≈ 6.6 for calcite dissolution at 25 °C and 1 atm. pressure concerning the *pH* dependency of the CO_3^{2-} concentration of water in equilibrium with air. Therefore, the aforementioned recommendation [40] can be considered rather optimistic. In permeation experiments calcite precipitation is also influenced by the crack width *w* and the water pressure *p* [11]. Both affect calcite growth indirectly through the *pH* change of the permeating water. Several crystallographic studies [41–44] confirm that the calcite growth rate is independent from flow velocity but decreases with increasing pH-value. Accordingly, a wider

crack and a higher hydraulic pressure leads to an increase of flow velocity, reducing the contact time of water with concrete and thus a less prominent increase of the pH-value. *Edvardsens* experiments confirmed this theoretical approach as absolute flow reduction was higher for 300 µm cracks than for 200 µm or 100 µm cracks. However, smaller cracks are more likely to close completely and show a higher relative flow reduction as volume flow is proportional to the third power of crack width ($Q \sim w^3$, comp. 4.3.2). Therefore, Eurocode 1992-3 [14] restricts crack widths and hydraulic gradients and set both in relation so that autogenous self-healing for water retaining concrete structures should be likely.

Additionally, calcite growth is often described as a two-phase kinetic process [11,17]. First, a fast surface-controlled growth of $CaCO_3$. Second, a slow diffusion-controlled growth since Ca^{2+} ions must diffuse through an already formed layer of $CaCO_3$ for further calcite growth. In the second phase the influence of crack width and hydraulic gradient on the flow reduction was found to be not relevant [11]. This perception was derived from characteristic volume flow curves as a function of time (see 4.3 for more details) [11], while also crack width measurements of specimens submerged in water revealed two phases of a crack closing rate [25]. However, in water immersion experiments the *pH* value of the water increases, and the carbonate ion concentration decreases with time and could therefore also impact calcite growth. Moreover, as of today, this model lacks directly determined growth rates and Ca^{2+} diffusion coefficients which would help to fully understand the healing process through calcite precipitation.

Moreover, calcite growth can be influenced by the water chemistry. In many cases water has no tap water quality when it permeates thru a separating crack in concrete structures. Thus, it is possible that water originates from soil or organic rich ground and contains increased quantities of dissolved organic matter (**DOM**). *Chave & Suess* [45] showed that DOM inhibits the growth of $CaCO_3$ by occupation of nucleation sites. Moreover, it was reported that phosphates and sulphates also inhibit calcite growth [46,47]. These findings could be reality in many construction environments and a decisive factor for the reliability of autogenous self-healing. However, these findings must be verified by experiments with through cracked concrete. Chemical monitoring of water permeating through cracks in real concrete constructions could help to enclose further inhibiting factors of calcite growth. However, a detailed review of the literature is necessary concerning chemical inhibition of calcite growth which is out of the scope of this study. The influence of seawater on calcium-carbonate formation is discussed in detail in chapter 4.4.

2.4 Blocking

This cause of autogenous self-healing can only apply when a fluid flows through a crack. Loose particles from the crack walls and/or particles in the permeating water can cause the clogging of flow paths whereas the blocking is likely to occur at bottlenecks of the three-dimensional crack geometry. The width of bottlenecks can be significantly influenced by the sieve line and aggregate size of concrete as further discussed in chapter 4.3.4. As published by *Clear* [9] in 1985, rapid flow reduction in the first seven days of permeation experiments is mainly due to this effect. However, without showing evidence. In contrast, *Edvardsen* [11] could not determine any sign of mechanical clogging in her experimental study and assigned the rapid flow reduction to the first stage of calcite formation (comp. 2.3 and 4.3). Yet, there is no study showing proof of the blocking of flow paths which generally could be a difficult task. Specimens must be prepared and cut in slices to allow an investigation of the crack interior. Thus, the probability of obtaining a slice showing evidence is low. Moreover, particles could loosen due to the preparation procedure. It is also likely that particles in blocked crack parts act as nucleation sites for calcite growth and are therefore overlooked. As of today, some authors still claim that blocking of flow paths is the main cause of early flow reduction [15]. Regarding the latter authors, this controversial statement could originate from experiments with water enriched in particles such as cement powder, bentonite or silica fume. In such experiments the leaking time is significantly reduced [11]. However, in practice it is often not possible to enrich water with particles. Moreover, this could be counterproductive in terms of calcite precipitation as the crack can partially fall dry behind a blocked part of the crack. If particles are loosened or washed out after a while autogenous self-healing processes could no longer be effective due to the hydration degree of the concrete [15]. Correspondingly, cracks could leak again.

3 Materials

The transmission of laboratory results to real concrete structures is difficult but should be a major goal to provide engineers with a reliable tool to assess the effectiveness of autogenous self-healing. However, cement-paste and mortar specimens of variable composition are frequently used to evaluate the effectiveness of autogenous self-healing as of today. Furthermore, different crack initiation techniques and adjusted crack widths can be found in the literature. This is discussed in the following chapters concerning the transferability of

laboratory results to real concrete structures. An overview of experimental design parameters of selected studies is given in **Table 10**. These parameters can be assessed by the reader after completing this chapter.

3.1 Specimen Properties

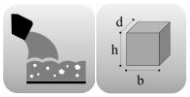

3.1.1 Sample size

The sample thickness should be based on real concrete component thickness, especially if permeability experiments are planned. When smaller specimens are conducted, results of the volume flow can be significantly influenced by inhomogeneities along the crack path (see 4.3 for more details). Moreover, constant carbonation of concrete specimens can result in a change of the microstructure and therefore of the self-healing ability. This effect can be expected to be more significant when small samples are used for experiments. According to the *DAfStb* standards, water retaining concrete constructions should have a minimum wall thickness of ≥ 240 mm (≥ 250 mm for bottom plates) [48]. However, the wall thickness must be greater when certain pressure gradients *I* and maximum water column heights h_w are exceeded. For h_w > 3 m ≤ 10 m, the concrete walls must be ≥ 400 mm < 660 mm. Respectively, a sample depth of 400 mm can be regarded as the minimum wall thickness of water retaining concrete components exposed to up to 1 bar water pressure. On construction sites, a limiting factor for autogenous self-healing can also be the crack length that can be > 1 m [10]. It is likely that such cracks are neither evenly permeated nor continuously healed and therefore remain leaky for a longer period of time or do not heal completely as observed in practice. However, crack lengths > 1 m are difficult to produce and to investigate in the laboratory. It is worth mentioning that the results of autogenous self-healing experiments have been extrapolated to cracks of arbitrary lengths to date, whereas only a few large scale experiments were carried out and remain to be verified [11,49]. Therefore, scaling experiments that aim at quantifying the effect of crack lengths and sample thickness on autogenous self-healing results could potentially lead to the introduction of a scaling factor to current self-healing criteria.

3.1.2 Number of specimens

Permeation experiments of cracked concrete show a considerable scatter of volume flow [11,22,50] (see 4.3 for more details). Even specimens with nearly the same surface crack width w_s tested under the exact same conditions can have completely different permeabilities due to variation of the 3-D crack geometry. Accordingly, the healing time and the volume flow can show a large

scatter. Therefore, several samples should be tested under the same conditions to obtain statistical relevance of the results. The initial flow, time to complete healing and/or the volume flow at the end of the experiment should be noted. *Van Mullem et al.* [50] suggest that at least 6 samples per test series should be conducted. Likewise, multiple specimens should be examined if permeation experiments are not planned.

3.1.3 Cement content

Some studies confirmed that continued hydration and calcium carbonate precipitation are restricted to the cement stone matrix [22,49] (comp. 2.2 and 2.3). The cement content influences the quantity of unhydrated cement particles that are exposed due to cracking and thus the ability of continued hydration to take place, while calcium carbonate formation could be promoted by the quantity of $Ca(OH)_2$. Accordingly, autogenous self-healing data of specimens with different cement content such as paste, mortar and concrete specimens are not comparable regarding the chemical causes of autogenous self-healing. Moreover, differences can also be expected for the swelling ability, the particles that form due to the cracking process and the crack geometry itself (**Figure 5**, see 4.3 for more details). From a practical point of view, concrete specimens should be used when tests aim at transferring laboratory results to real structures. For this purpose, the cement content of concrete mixes should be within the range of the applicable standard and exposure conditions [3]. For water-retaining concrete structures, a minimum cement content of ≥ 280 kg*m^{-3} is recommended according to the German board for reinforced concrete structures (DAfStb) standard [48]. Regarding DIN EN 206-1 [51] and DIN 1045-2 [40], this minimum cement content must be further increased under certain exposure conditions.

3.1.4 Cement type & Supplementary cementitious materials

According to *Edvardsen* [11], the cement type, pozzolanic, latent hydraulic supplementary cementitious materials and other additives that affect the availability of Ca^{2+} such as fly ash, ground blast furnace slag or limestone powder do not affect the extent of autogenous self-healing, respectively the calcite precipitation. However, this finding is controversially discussed in the literature (comp. 2.2 and 2.3). Therefore, *Edvardsen*s results should be verified on modern cements, which typically have a reduced clinker content. As of today, cement types are not restricted by code regulations that consider autogenous self-healing of through cracks.

3.1.5 Aggregate volume & Sieve line

The tortuosity and effective crack length of thru cracks in cementitious materials are significantly influenced by both aggregate volume and sieve line [10,12,13]. Accordingly, permeability and autogenous self-healing of cement paste, mortar and concrete are not

comparable (see 4.3 for more details). A similar argumentation accounts for concrete samples with different aggregate volumes and sieve lines since tortuosity superimposes the general high scatter of permeability experiments. Therefore, sieve line and maximum aggregate size should be held constant within a test series and in the range of the applying code. According to DAfStb standard [48] for water retaining concrete the maximum grain size is restricted to ≤ 32 mm for a wall thickness of 400 mm.

3.1.6 W/C ratio

According to the DAfStb standard [48] for water retaining concrete structures, the *W/C* ratio should be ≤ 0.60 for a structural thickness of 400 mm. When seawater exposure applies the max. *W/C* ratio should further be restricted to ≤ 0.45 for XS3 and ≤ 0.55 for XS1 according to DIN EN 206-1 [51] and DIN 1045-2 [40]. It is also reported that the tortuosity of cracks in cementitious materials decreases with decreasing *W/C* ratio [52] (see 4.3 for more details). Moreover, a low *W/C* ratio leads to less hydrated cement (comp. 2.2), which may affect autogenous self-healing by continued hydration [53]. Therefore, for reasons of transferability to real concrete structures, the *W/C* ratio should be in the range of the applicable standard and kept constant within a test series.

3.1.7 Concrete age

The testing age, respectively the hydration degree of concrete specimens can have a significant effect on the efficiency of autogenous self-healing. It has been reported that autogenous self-healing is most effective for young concretes [54–56]. However, current code regulations [14,40] do not restrict autogenous self-healing to cracks that form solely by early age crack formation e.g., due to shrinkage. *De Belie et al.* [17] reviewed studies attributing the deceasing healing efficiency to the increasing amount of CSH phases formed over time due to the slow pozzolanic reaction. This argumentation is based on the lower solubility of CSH compared to $Ca(OH)_2$ which could limit the availability of Ca^{2+} for calcium-carbonate precipitation at higher hydration degrees. However, this contradicts with results of other studies that showed that autogenous self-healing is independent of the cement type and cementitious supplementary materials [10,11], as both affect the initial CH and CSH concentration. Accordingly, it remains unclear which explicit process limits the efficiency of autogenous self-healing at higher concrete age. Therefore, systematic experiments with different sample ages should be performed. It is worth noting that most reviewed publications started with permeation experiments after 28 days of curing (Table 10). In practice, concrete structures are also frequently exposed to water after 28 days of curing.

3.2 Crack Initiation & Crack Width

Autogenous self-healing approaches can be applied when water retaining concrete structures show early load-independent cracking, which is mainly due to constrained stresses resulting from temperature profiles within the concrete element, plastic-, drying-, chemical- and autogenous shrinkage [4,11,57]. When through cracks are formed the constrained stress shows a uniform tensile-stress distribution [4,58]. Generally, the crack generation technique impacts the crack geometry due to different stress states [59]. Since the permeability of cracked concrete is sensitive to the crack geometry (see 4.3 for more details) results of permeability experiments are affected by the cracking technique. Therefore, cracks in laboratory concrete should be initiated according to the stress state of the cracking mechanism. Moreover, it is unlikely that crack walls rotate in real constructions after cracking. Thus, the parallelism of crack walls should always be given to conserve the initial crack geometry. This is not the case when the initial crack width is readjusted, or specimens are put back together after cracking. In general, crack widths should be in the range of 100 µm, 200 µm and 300 µm as these are the restricted widths by *Eurocode 1992-3* [14]. However, it must be mentioned that in reality cracks in concrete often show a branching that can reduce the spatial crack width and increase the crack length which could promote autogenous self-healing. Accordingly, different fibers and reinforcement close to the surface were tested in different studies [11,12,17,60,61]. *Edvardsen* found that steal fibers increase the surface crack width. In her study, only reinforcement close to the surface promoted crack branching and was effective in reducing the initial flow and the healing time but was dependent on the degree of reinforcement. On the other hand, it was reported that fibers reduce the permeability by up to 90 % and reinforcement only by 30 % [12]. However, the effect was found to depend on the fiber type (steal, polyacrylonitrile, polyvinyl-alcohol (**PVA**)) and the volume of fibers. In addition, *Mechtcherine et al.* [61] reported that finer fibers (glass and carbon fibers) lead to the formation of finer but more cracks. Also the precipitation of $CaCO_3$ is influenced by the presence of fibers (PVA) which act as nucleation sites [60]. However, further systematic experiments are desirable. Moreover, the coefficient of variation (COV) of the measured mean surface crack width of a test series should be < 4 %, if one aims at assessing the effect of different crack geometries on permeation [50]. Variation of the initial flow of samples can then be assigned to variation of the crack geometry. In the following paragraphs commonly applied cracking techniques (**Figure 3**) are discussed according to the aforementioned requirements. An overview of the pros and cons in given in **Table 1**.

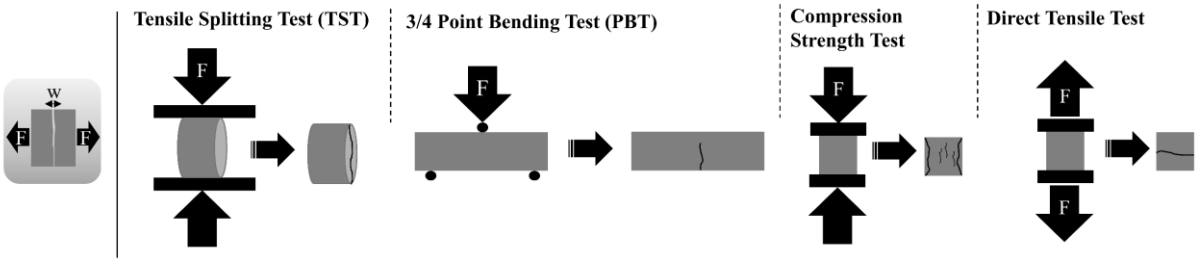

Figure 3. Schematic overview of common crack initiation techniques.

In most recent publications cylindrical specimens were cracked by **tensile splitting test (TST)** [22,25,29,30,62–65]. This method is easy to use, fast, and has a uniform tensile-stress distribution according to simulations [66], while only the margins subjected to loading show small areas of compressional stress regimes that most authors consider negligible. However, crack width must be monitored by linear variable displacement transformers (**LVDT**) during crack initiation to stop loading when the desired width is reached, while cracks can then partially close again after unloading by up to 32 % to 72 % [67]. Furthermore, it was reported that cracks open on one side and then propagate thru the sample, which is why the crack width must be controlled on both flat sides of the cylinder during a TST [62]. Respectively, the tensile stress distribution is not as uniform from a practical point of view. Moreover, it is likely that rotation of the crack walls occurs when the crack width is readjusted after crack initiation or crack walls "snap-back" due to unloading. This can cause the clogging of flow paths due to wedged particles or crack surfaces and should be avoided in permeation experiments. However, this is not important when specimens are simply submerged in water for healing. To protect samples from breaking apart the cylinders can be coated by epoxy or other reinforcing materials such as done by *Van Tittelboom et al.* [29].

Alternatively, **3/4 point-bending tests (PBT)** are recommended by some studies [59,68]. This method is also easy to use and fast but shows a non-uniform tensile-stress distribution as compressional stresses apply on the loading face. Mostly lab sized prismatic samples are cracked with this method, whereas for instance *Danner et al.* [69] used PBT-techniques to initiate cracking on several meter long concrete beams. However, it can be difficult to keep the specimen attached after cracking. Therefore, a thin coating of carbon fiber plastic can be applied on the loading face to protect the samples from breaking apart as reported by some authors [50,70,71]. In other studies [19,27,53], the specimens were only pre-cracked to avoid breaking apart, which means that the loading was stopped as soon as a small crack tip opened. With the latter, crack width reduced after unloading [53,70]. For plastic coated specimens crack width must be readjusted after crack initiation, whereas for completely separated specimens the crack must be

reassembled. Therefore, rotation of crack walls is unavoidable with the consequences for permeation experiments that were outlined above. For active crack width control special retainers are widely used [7,50,69,70]. However, it was reported that elastic creep of readjusted cracks can lead to the partial closure of the opening with time, while the absolute extent of elastic creep depends on the exact restraining method [50]. Therefore, relaxation time and the extent of elastic creep should be monitored before self-healing or permeation experiments are carried out to eliminate this effect. Another approach is to fix crack width by applying an epoxy coating such as done by *Yuan et al.* [19]. Epoxy coatings show negligible elastic creep, but special care must be taken to ensure that the resin does not flow into the crack. Generally, it is rather unusual to perform permeability tests with prismatic specimens that were cracked by PBT, while most studies use such specimens for self-healing experiments in water immersion. However, *Van Mullem et al.* [50] and *Gruyaert et al.* [70] proposed a special permeation test setup with active crack width control that was also tested in a round-robin test series [71]. Prismatic (160x40x40 mm^3) samples are coated by a carbon fiber plastic on the loading side, crack width is readjusted and restrained after crack initiation and the crack sides are sealed with methylacrylate. Water flows then through a hole in the center of the sample, before entering the crack. A major disadvantage of this method is the increased contact time of water with concrete due to the flow path thru the half length of the specimen before entering the crack. This can influence autogenous self-healing due to an increased *pH* value and increased Ca^{2+} availability in the water. Moreover, the triangular crack shape of this method produces bottlenecks at the narrowest part. This method might be suitable for short permeability experiments, for instance to investigate the impact of crack geometry on permeability but is not suitable for long time autogenous self-healing experiments due to the disadvantages outlined above.

Another approach are **compressive strength tests** for crack initiation. This method can be considered completely unsuitable for crack initiation as the stress distribution is contradictory to the requirements mentioned above. Moreover, specimens often show multiple cracking, displacement and deterioration after the test. Furthermore, it is not possible to fix or adjust crack widths. Therefore, the extent of healing cannot be compared to the initial crack width and thus the extent of healing cannot be assessed.

Direct tensile tests are rather uncommon for crack initiation. However, this method provides pure tensile stress, while the biggest disadvantage is the complete separation of the specimen after cracking or the partial closure of cracks after unloading [61]. Respectively, the sample must be reassembled, and the crack width readjusted, or the flow path can be blocked due to the "snapping back" of the crack walls. Moreover, for large scale specimens' custom setups are

needed. However, the mechanism of crack initiation is the most realistic one regarding early load-independent cracking. *Edvardsen* [11] developed an experimental setup based on the latter crack inducing technique (**Figure 4**). To avoid an uncontrolled separation of the sample or "snapping back", the tensile stress is applied in small steps by rotating nuts on threaded rods that simultaneously act as crack width retainers. The tensile force is brought into the concrete through cast in curved threaded rods, while thick metal plates at the back side of the concrete specimen provides sufficient counter force. However, it is important to allow for relaxation after each step of increasing the tensile stress until crack initiation. The exact location of cracking is then given by notches in the specimen that result from the special casting framework.

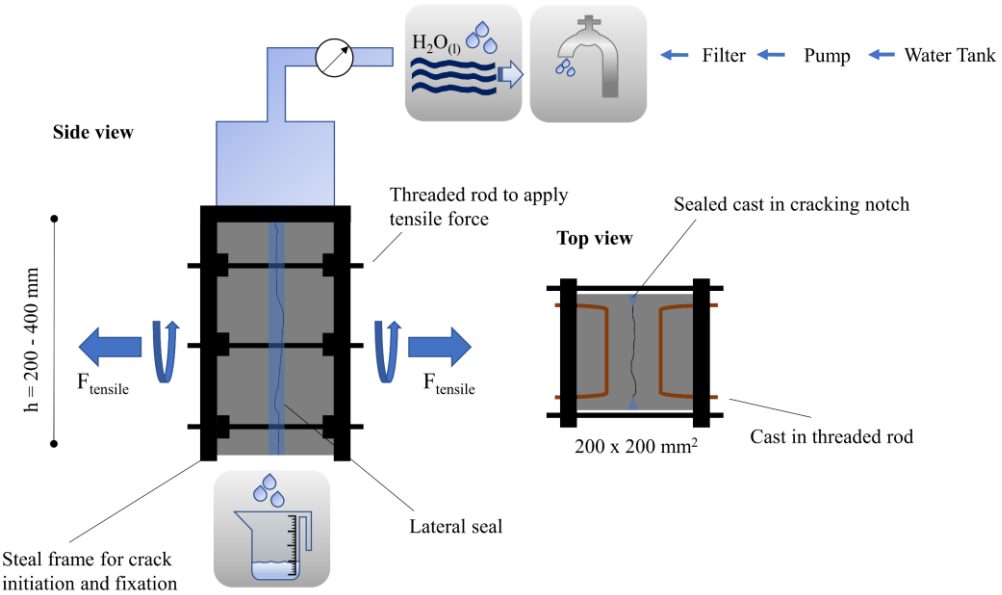

Figure 4. Schematic illustration of the experimental setup used by *Edvardsen* [11] to investigate the efficiency of autogenous self-healing of cracked concrete.

The greatest advantage of this setup is the maintained parallelism of the crack walls that are hold in position during the crack initiation. The greatest disadvantages are the complexity and time-consuming crack initiation. Furthermore, the size of the setups must be varied when scaling experiments are aimed at. However, this setup can be used as a framework for concrete casting, crack initiation and permeability experiments. However, stress rates and relaxation times are not given in *Edvardsens* study and therefore must be approached by trial and error in further research following this test design.

Table 1. Overview of advantages and disadvantages of different crack initiation methods.

Crack Initiation	Crack Type	Advantages	Disadvantages
Tensile Splitting Test (TST)	Separating crack	• Almost pure tensile stress. • Practicability. • Easy upscaling of the sample dimensions. • Crack Type.	• Rotation of crack walls. • "Snapping back". • Multiple cracking.
3/4-Point-Bending-Test (PBT)	Bending crack	• Practicability. • Easy upscaling of the sample dimensions.	• Rotation of crack walls. • "Snapping back". • Compressional stress. • Crack Type.
Compressional Stress Test	Cracking due to excessive loading	• Practicability. • Easy upscaling of the sample dimensions.	• Compressional stress. • Deterioration of the sample. • Multiple cracking. • Crack type.
Direct Tensile Test	Separating crack/early cracking	• Pure tensile stress. • Crack type.	• Rotation of crack walls. • Custom setup for large scale specimens.
Cracking according to Edvardsen	Separating crack/early cracking	• Pure tensile stress. • Parallelism of crack walls. • Crack type. • Casting, Cracking and Permeation in one setup.	• Custom and complex test setup. • Expansive and time-consuming scaling experiments.

4 Influence of Different Exposure Conditions on Autogenous Self-Healing

After working in the process theory of autogenous self-healing, material selection, casting, curing and cracking of the specimens, the samples must be exposed to a healing environment to initiate autogenous self-healing (**Table 2**).

Table 2. Overview of commonly applied exposure conditions to initiate autogenous self-healing, variables of the experimental setup and typical assessment method of the healing efficiency.

Healing Environment	Variables of the experimental setup	Assessment of the healing efficiency
1. Submersion in Water 	• Water chemistry and temperature. • Gas exchange. • Healing Period. • Sample composition, dimensions and crack width.	• Surface crack width measurement • Short permeation experiment.
2. Wet & Dry Cycles 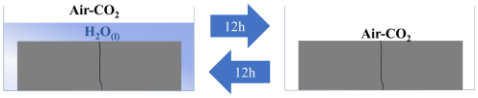	• Water chemistry and temperature. • Container volume. • Healing period. • Sample composition, dimensions and crack width.	• Surface crack width measurement.
3. Permeation Experiment 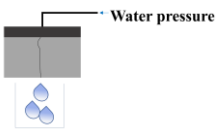	• Water chemistry, temperature and pressure. • Healing period. • Sample composition, dimensions and crack width.	• Volume flow as a function of time.
4. Humidity Chamber 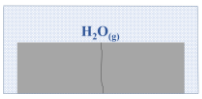	• Temperature and pressure. • Healing period. • Sample composition, dimensions and crack width.	• Surface crack width measurement.

The healing environment, its possibilities and limitations should be clarified in advance of any experiment to avoid disturbance of the workflow. In addition, it is particularly useful for the reader of self-healing literature to be aware of different exposure conditions and corresponding experimental variables that can affect autogenous self-healing results to avoid misinterpretation of experimental data. In the following chapters an overview of commonly applied exposure conditions is given, and the possibilities and limitations are discussed.

4.1 Submersion in Water of Through Cracked Concrete Specimens

In many studies [19,30,31,39,72,73] cracked concrete specimens are submerged in water to investigate the extend of autogenous self-healing for the sake of simplicity. Therefore, instead of measuring the permeability, surface crack width measurements are mostly carried out. Thus, watertightness cannot be accessed (Figure 5) and only swelling, continued hydration and calcite precipitation apply in these experiments. Only in a few studies [22,30] healing was initiated in water immersion experiments and the watertightness tested after defined healing periods in permeability tests. These experiments only allow for blocking of the crack during the water tightness evaluation. Moreover, the healing process is terminated as the samples are moved into a permeability setup. This provides multiple error sources such as change of the crack width, contact to atmospheric CO_2 etc. Respectively, it is difficult to compare results with continuously permeated concrete specimens. The main mechanism of autogenous self-healing of samples immersed in tap water under atmospheric conditions is the precipitation of calcite [18,72]. However, only little is known about the impact of the container size, respectively the water volume on the temporal availability of relevant carbonate ions and *pH* development during such experiments. Both could affect the self-healing results (comp. 2.3). *Maes* [20] showed that samples submerged in deionized water exhibit a much slower self-healing rate as mainly continued hydration applies. However, it is not clear from the authors study whether the experimental setup was exposed to atmospheric conditions. One can conclude that carbonate species must be present in the water for calcite precipitation to take place and the kinetics of dissolution of CO_2 in the water is too slow to be recognized by the experiment. When the samples are submerged in artificial seawater the self-healing mechanism changes (see 4.5 for more details). All immersion tests in tap water have in common that calcite precipitation mainly takes place at the surface of the specimen adjacent to the crack opening and not in the sample interior. This seems to depend on the initial crack width, since 200 µm cracks show $CaCO_3$ at

the crack opening while 400 µm cracks show $CaCO_3$ precipitates along the whole crack path [30,31]. On the other hand, permeation experiments by *Edvardsen* [11] showed calcite precipitation along the whole crack path regardless of the crack width. Thus, due to the lack of motion in water immersion experiments there must be a depletion of relevant ions inside of the crack. A mechanism is proposed by *Palin et al.* [30]. Respectively, carbonate species quickly deplete in the interior which leads to the formation of a concentration gradient and the movement of Ca^{2+} ions towards the crack opening. Therefore, excessive calcite precipitation takes places at the concentration front. However, the depletion of carbonate ions is only effective for crack widths ≤ 200 µm.

4.2 Cyclic Submersion in Water of Through Cracked Concrete Specimens/Wet & Dry Cycles

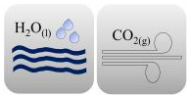

It was reported [18,20,22,60,72] that the self-healing rate in the first days of a healing process is faster with cyclic water immersion and drying periods (typically repeated cycles of 12 hours water immersion 12 hours air exposure) compared to continuous water immersion. Generally, swelling, continued hydration and calcite precipitation are the only causes of self-healing that apply in these experiments. However, the main mechanism of self-healing remains the precipitation of calcite when tap water in equilibrium with atmosphere is used for healing. Calcite precipitates at the crack opening (comp. 4.1) whereas the interior mainly shows continuous hydration [60]. According to *Maes* [20], calcite precipitation at the crack opening is accelerated due to the direct contact of the concrete to atmospheric CO_2. However, it is not addressed that the solubility of calcite could also be exceeded due to evaporation of water on the specimen's surface and therefore lead to the faster precipitation of calcite in the beginning of the healing process. Interestingly, the absolute extend of self-healing remains controversial. According to *Roig-Flores* et al. [22,72], cyclically submerged specimens exhibit a lower maximum healed crack width after a healing period of 42 days compared to continuously submerged samples although healing was faster in the first 7 days. *Suleiman et al.* [18] could not determine any difference after 9 month. Thus, the healing period itself can be addressed as a possible reason for the contradictory results. Especially for the second, diffusion-controlled phase of calcite growth, the constant availability of the transport medium water could be beneficial (comp. 2.3). Therefore, controlled wet & dry cycles are only of interest to simulate the influence of tidal zones on autogenous self-healing in cracked concrete but not for

application as a healing accelerator on construction sites. Moreover, from a practical point of view, it is important that cracks carry water continuously as uncontrolled dry periods can stop the self-healing process (comp. 2.1 and 4.4).

4.3 Permeation of Through Cracked Concrete

In many concrete structures such as underground garages or water tanks concrete walls hold back water on one side to ensure the functionality of the construction. Thus, separating cracks are permeated when water pressure applies to only one side of the wall (Figure 5). In such a situation all causes of autogenous self-healing apply simultaneous, since the blocking of flow paths with particles is only possible when specimens are subjected to water flow. Typically, permeation curves exhibit a rapid decrease of volume flow in the first ~ 48 hours of exposure, while at later stages a minimum is asymptotically approached [10,11,15,63,74]. When freshwater in equilibrium with air permeates through a crack, calcite precipitation is the main mechanism of healing and deposits along the whole crack path, whereas the healing effectiveness depends on the initial crack width and the hydraulic gradient [11]. Accordingly, a two-stage model of the kinetics of calcite growth is often concerned (comp. 2.3).

Gruyaert et al. [70] found that increasing the water pressure from 0.05 bars to 2 bars on cracks that were already healed can cause the cracks to leak again. *Reinhardt & Jooss* [64] showed that flow reduction is most effective at higher temperatures of the permeating fresh water (up to 80 °C). This can be explained by the decreasing solubility of calcite with increasing temperature and a higher flow velocity due to a decreased viscosity of the water (comp. 2.3). Thus, the increase of the *pH* of the permeating water is less pronounced and the calcite growth rate is higher. Furthermore, there is a greater supply of ions due to a higher flow rate. T*sukamoto & Wörner* [12] investigated the effect of viscosity of different fluids such as different hydro carbons on autogenous self-healing. In this way the influence of continued hydration and carbonation could be excluded and limited to swelling and blocking of the flow path. Interestingly, the authors found that for liquids with a lower viscosity than water self-healing can only be expected for crack width < 100 µm. Therefore, it can be concluded that the effectiveness of blocking of flow paths is highly dependent on the viscosity of the permeating fluid. Other permeation experiments were carried out with fresh water of different hardness [10,11], deionized water [18,20,25,29,53] and synthetic seawater [20,30,31]. Water hardness was found to have no influence on the extent of self-healing. The use of deionized water causes mainly continued

hydration. When synthetic seawater is used the mechanism of the chemical causes of autogenous self-healing change (see 4.5 for more details).

In general, two approaches can be differentiated to describe water flow thru cracked concrete. First, permeation thru a homogeneous and porous medium according to Darcy (see 4.3.1 for more details). Second, permeation thru a smooth gap according to Hagen-Poiseuille (see 4.3.2 for more details). Both are discrete solutions of the partial differential Navier-Stokes equations which describe the motion of viscous fluids and thus can be used to investigate permeation of water through bulk concrete, cracked concrete and the extend of self-healing of cracked concrete. In most experiments, cracked concrete specimens are permeated from top to bottom or bottom to top by a uniform fluid flow. However, *Meichsner & Röhling* [15] point out that the assumption of a uniform flow thru the crack, continuous reduction of the flow effective cross section through autogenous self-healing and the universal transfer of laboratory results to real structures are a risk in the design rules.

4.3.1 Permeation According to Darcy´s Law

The Darcy law describes the laminar flow of a viscous fluid through a porous medium and was derived by experiments from Henry Darcy in 1856. In case of uncracked concrete, water permeates through an irregular network of pores, while the cement stone, aggregates and reinforcement are considered impermeable. The flow paths are complex and accompanied by dispersion and diffusion. As a simplification the filter velocity v_F (**Equation 1**) is formulated that is defined as the quotient of volume motion per second Q [m³*s^{-1}] and cross-sectional area A [m²] [75,76].

$$v_F = \frac{Q}{A}\ [m * s^{-1}] \qquad \textbf{Equation 1}$$

The filter velocity is proportional to the hydraulic gradient I [-] (basically the difference of the water column height at point 1 (h_1 [m]) and 2 (h_2 [m]) separated by the length l [m]) and the hydraulic conductivity-coefficient k_f [m*s^{-1}] (**Equation 2**) which is defined by the pore volume, pore connectivity and the granular network K [m²] as well as density ρ [kg*m^{-3}], gravity g [m*s^{-2}] and dynamic viscosity η [Pa*s] of the permeating fluid [75,76] (**Equation 3**).

$$v_F = \frac{Q}{A} = k_f * \frac{h_1 - h_2}{l} = k_f * I\ [m * s^{-1}] \qquad \textbf{Equation 2}$$

$$k_f = \frac{K * g * \rho}{\eta}\ [m * s^{-1}] \qquad \textbf{Equation 3}$$

The following condition of the experimental setup must be met in order to apply Darcy´s Law [65,77,78]: a) the specimen is completely saturated with the permeating fluid, b) both

specimen surfaces are in contact with the permeating fluid, c) flow is laminar, d) the fluid is incompressible and e) the hydraulic gradient is only consumed for flow thru the crack or interior of the sample.

Hydraulic conductivity of cement paste is reported with 10^{-15} bis 10^{-12} [m*s^{-1}] [79–81], while *Nokken & Hooten* [81] state that this range is also valid for mortar and concrete. In contrast, *Wang et al.* [63] gives conductivity-coefficients for concrete in the range of 10^{-12} to 10^{-11} [m*s^{-1}]. A detailed discussion of the controversy is given by *Wu* [82,83], who also reported a more complex distinction of parameters influencing the permeability of cementitious materials. Thus, a) a reduction of cement paste volume, porosity, increased tortuosity by aggregates reduce the permeability, b) densification of the cement matrix by incorporation of ground blast furnace slag and limestone powder reduce permeability, c) the presence of interfacial transition zone between cement stone and aggregates (**ITZ**) and d) connectivity of ITZ increases permeability [59]. Furthermore, the influence of aspects c) and d) increases rapidly with volume of aggregates. For an aggregate volume > 35 % it is reported that the impact of the ITZ exceeds permeability reducing aspects such as the densification or pore reduction [83]. The increase of hydraulic conductivity-coefficients of cement paste, mortar, normal strength concrete (**NSC**) to high strength concrete (**HSC**) measured by *Aldea* et al. [62,67] with associated aggregate volumes of 0 %, 50 %, 74 % and 77 % agrees with these results.

Darcy´s Law is also applied to fractured rocks or concrete with thru cracks [25,29,62,63,65,67,74,78]. When it comes to flow thru cracks the rock or concrete matrix and the crack surfaces are considered impermeable. Thus, as an approximation the fluid flow occurs only thru the crack. A comparison of the hydraulic conductivity-coefficients of cracked and uncracked concrete shows that this assumption is correct. For cracked concrete with a crack width of 300 to 400 µm, k_f is given in the range of 10^{-4} bis 10^{-5} [m*s^{-1}] [62,63]. A similar argumentation accounts for transport by diffusion and capillary suction [59]. *Wang et al.* [63] and *Aldea et al.* [62,67,74] investigated the influence of different crack widths on the hydraulic conductivity k_f. According to *Wang et al.* the influence of cracks is only significant for $w \geq 50$ µm with a slightly increased conductivity coefficient of 10^{-10} [m*s^{-1}] compared to uncracked concrete. However, the author only investigated one concrete specimen per crack width. Furthermore, the crack length l orthogonal to the flow lines was variable and not recorded by measurements. *Aldea et al.* report that the increase of conductivity-coefficient is only significant for $w \geq 100$ µm although a similar test setup was used. As already highlighted by *Mengel et al.* [59] critical crack widths $w_c << 50$ µm for water permeation are reported by other authors [20,84–86]. For instance, $w_c \approx 10$ µm is reported by *Louis* [84]. Interestingly, the same w_c for chloride penetration is reported by

Maes [20]. Differences might be due to different experimental setups, hydraulic gradients and measurement techniques of the crack width used by different authors. For instance, crack widths measured with electrical displacement transformers such as linear variable displacement transformers **(LVDT)** include the crack processing zone in the measurements. This technique consistently overestimates the crack width by 30 to 100 µm compared to optical measurements [16,87]. Another study reports an overestimation by the factor of 2.5 [86]. Unless the controversy about w_c it can be concluded that for crack widths restricted by Eurocode 1992-3 [14] permeability is predominated by the crack.

Beside the crack width *w*, crack length orthogonal to the flow direction (*l*) is listed by *Wang et al.* as an influencing factor on the conductivity coefficient whereas the need for further research was pointed out by the authors as *l* was variable in the experiments but not systematically measured. Crack length parallel to the flow direction (*d*), respectively the sample thickness is reported by *Aldea et al.* [62] to have little to no influence on k_f. That this is not the case is shown in chapter 4.3.2 in detail. Additionally, it must be added that both *Aldea et al.* and *Wang et al.* investigated only a few samples and the specimen's diameter and thickness was very small (Table 10). Generally, it is recognizable that in permeability self-healing studies of the past decade, sample size and dimension stayed small. Thus, results are likely influenced by inhomogeneities along the crack paths (Figure 5).

4.3.2 Permeation According to Hagen-Poiseuille

The Hagen-Poiseuille equation (**Equation 4**) was derived experimentally by Poiseuille and Hagen in the mid-19th century. It describes the laminar flow of a viscous, incompressible fluid thru a smooth gap [75,88]. However, cracks in concrete exhibit a variable crack width over sample width and depth, tortuous crack geometry and rough crack surfaces. Hence, the Hagen-Poiseuille Equation would overestimate flow through separating cracks in concrete. Respectively, the correction factor ξ was introduced by several authors (**Equation 5**).

$$Q_{smooth} = \frac{\Delta p * w^3 * d}{l * 12 * \eta} = \frac{g * I * d * w^3}{12 * \nu} \; [m^3 * s^{-1}] \qquad \textbf{Equation 4}$$

, with $\Delta p \; [Pa] = \rho \; [kg * m^3] * g \; [m * s^{-2}] * \Delta h \; [m]$ and $I \; \frac{\Delta h}{l}$.

$$Q_{concrete} = \xi * \frac{g * I * d * w^3}{12 * \nu} \; [m^3 * s^{-1}] \qquad \textbf{Equation 5}$$

As previously mentioned, studies following the Darcy approach already showed a dependency of the crack width *w* [m] on permeability. The rapid increase of hydraulic conductivity coefficients with *w* can be assigned to the fact that volume flow *Q* is proportional to the third power of *w* which was confirmed among others by *Edvardsen* [11]. The influence of hydraulic

gradient *I* [-], crack length *l* [m] (orthogonal to flow) and *d* [m] *(*parallel to flow*)* and viscosity (dynamic viscosity η [Pa*s] or kinematic viscosity v [m^2*s^{-1}]) of the fluid on volume flow become clear with reference to the Hagen-Poiseuille equation. The consequences for calcite precipitation are addressed in chapter 2.3.

However, in practice the three-dimensional crack width, tortuosity and roughness show a significant scattering. Experiments with the same experimental design parameters and similar measured surface crack widths can result in totally different ξ values. Therefore, different approaches and ranges of ξ values can be found in the literature (**Table 3**). Constant ξ values in the range of 0.125 to 0.25 are proposed by *Edvardsen* [11], *Meichsner* [10] and *Clear* [9]. *Tsukamoto & Wörner* [12] and *Ripphausen et al.* [13] suggest a variable correction factor depending on the sieve line and crack width. *Louis* [84] introduced a correction factor depending on the relative roughness $\boldsymbol{K/D_h}$. With K the absolute roughness and D_h the hydraulic diameter that is equal to two times *w*. Lately another approach was issued by *Akhavan et al.* [86] building on *Louis* results. The authors propound to include a tortuosity factor *T* determined by the mean height of crack surface asperities and the effective length of the crack. The authors found ξ in the range of 0.163 to 0.229 which is in accordance with *Edvardsens* results.

However, it must be noted that the experiments of *Akhavan et al.* [86] were carried out on mortar samples with a diameter of 89 mm and a thickness of only 25 mm. Thus, this approach needs to be verified on thicker concrete specimens. Yet, for real concrete structures it is impossible. However, it is proof for the widely accepted influence of crack geometry, roughness and tortuosity on permeability of cracked cement-based materials. Compare chapter 4.3.4 for a detailed discussion of the influencing factors on crack geometry, roughness and tortuosity.

Table 3. Overview of different correction factors ξ of selected authors.

Author	Correction factor ξ [-]
Edvardsen (1996) [11]	$\xi = 0.25$
Ripphausen (1989) [13] and Clear (1985) [9]	$\xi = 0.125$
Louis (1967) [84]	$\xi = \frac{1}{(1 + 8{,}8 * (K/D_h)^{1{,}5})}$
Akhavan et al. (2012) [86]	$\xi = \frac{T}{(1 + 8{,}8 * (K/D_h)^{1{,}5})}$

4.3.3 Characteristics of Flow Through Cracked Concrete

The introduced flow models (comp. 4.3.1 and 4.3.2) describing the permeability of cracked concrete are only valid for laminar flow [75,88]. To evaluate the flow regime the Reynolds number *Re* [-] can be calculated (**Equation 6)**. In case of fluid flow thru a gap *Re* depends on the volume flow *Q* [mm^3*s^{-1}], crack length ***l*** [mm] and kinematic viscosity $\boldsymbol{v}$ [mm^2*s^{-1}] of the fluid [65].

$$Re = \frac{\bar{V} * D_h}{\nu} = \frac{Q * 2 * w}{A * \nu} = \frac{2 * Q}{l * \nu} \; [-]$$ **Equation 6**

For *Re* < 2300 flow is laminar. For 2300 < *Re* < 3000 a transmission zone is stated, whereas for *Re* > 3500 flow is purely turbulent [65,75,88]. To distinguish between parallel and non-parallel flow the relative roughness must be considered. According to *Lomize* [11,89] flow is parallel for $K/D_h < 0.032$, whereas above this value non-parallel flow is present which still can be laminar. Concerning *Louis´s* Equation (Table 3) and applying $\xi \approx 0.25$ as suggested by *Edvardsen* a relative roughness of ≥ 0.48 can be calculated for thru cracks in concrete. Thus, fluid flow thru cracked concrete in general is non-parallel. Furthermore, transition from laminar to turbulent flow regimes occurs at lower *Re* values with increasing relative roughness [75]. For $K/D_h \approx 0.5$ a critical *Re* of 450 can be calculated according to *Rissler* [75,90]. To approximate the transition of the flow regime as a function of hydraulic gradient I_c [-], crack width *w [m]* and kinematic viscosity *v* [m^2*s^{-1}] of the fluid and gravity *g* [$m*s^{-2}$], the following equations for non-parallel and parallel flow are given by *Wittke* [75] (**Table 4**).

Table 4. Critical hydraulic gradient for the transmission from laminar to turbulent for parallel and non-parallel flow [75].

Flow Condition	Critical Hydraulic Gradient I_c [-]
Non-parallel - $K/D_h \geq 0.032$	$I_c = \frac{11000 * v^2}{g * w^3}$
Parallel - $K/D_h < 0.032$	$I_c = \frac{13800 * v^2}{g * w^3}$

Applied to crack widths according to the restrictions of Eurocode 1992-3 [14] it can be seen that the transition from laminar to turbulent flow occurs at rather high hydraulic gradients. For a common structural thickness of 400 mm this results in a critical pressure of ~ 1.6 bars for 300 µm, ~ 5.5 bars for 200 µm and ~ 44.2 bars for 100 µm cracks (calculated with a kinematic viscosity at 20 °C of $1.002*10^{-6}$ [m^2*s^{-1}], check Equation 4 for the conversion of the hydraulic gradient *I* to pressure *p*). These pressures should not be exceeded in experiments and are unlikely to be reached in realistic construction environments [11,84].

Furthermore, for *w* > 300 µm and *Re* > 100 *Shin et al.* [65] propose the calculation of the true water head accounting for head losses due to the experimental set up. Above the critical *Re* and *w* a variation of up to 40 % of the applied water head was determined due to the energy losses causes by the change of flow lines in the experimental setup. Accordingly, permeation results of specimens with $w_{max} > 300$ µm obtained with different test-setups are not comparable regardless of the composition and crack geometry. Therefore, the limitation to cracks widths ≤ 300 µm can be formulated as a design criterion for future experiments.

4.3.4 Crack Geometry, Roughness and Tortuosity of Through Cracks in Concrete

In the previous chapters it was shown that fluid transport through concrete with a separating crack is mainly characterized by the crack itself. The precise crack geometry, roughness and tortuosity restrict the volume flow and are often summarized in the correction factor ξ following the Hagen-Poiseuille approach. However, these flow reducing parameters scatter severely even when the same experimental design was used [11]. Furthermore, crack geometry, roughness and tortuosity are influenced by variables of concrete mixtures and design criteria. For instance, crack geometry can be strongly influenced by the aggregate size due to grains that partly stand out of the crack surfaces. This effect can locally reduce the crack width and provide bottlenecks for the blocking of the flow path and nucleation of calcite [10,12]. At the same time the flow path becomes more tortuous, respectively the effective crack length $l_{effctive}$ increases [12,13,86] (**Figure 5**). On the other hand, it was reported that higher *W/C* ratios reduce tortuosity [52]. Therefore, it is difficult to compare experimental results when aggregate size, sieve line and/or *W/C* ratio are different and superimpose on the generally high scattering of permeability tests. In real concrete structures the reinforcement plays another important role. It was shown by several studies that crack width decreases at the bars [91–93] whereas the crack width at the surface is generally wider but dependent on the concrete cover [93,94]. Accordingly, *Akhavan et al.* [86] reported for mortar samples without reinforcement that the surface crack width is 13 % greater than the interior crack width. However, the latter authors investigated only one cross section of the crack per sample and results must be verified on concrete specimens. In general, it is difficult to find reliable data of the crack width in the interior of concrete specimens as a function of composition. Moreover, there is a lack of a calculation method that allows to estimate the crack geometry as already stated by *Mengel et al.* [59]. Thus, concerning the transmission of laboratory results to real structures, concrete composition (cement type, aggregates, *W/C* ratio, etc.) [10,12,13,52], degree and assemblage of reinforcement and concrete cover [13,92–94] need to be considered and carefully documented. As a matter of fact, most studies on autogenous self-healing did not investigate the crack width in the interior of the samples but only considered surface crack width. This is due to the problem that crack width measurements in the interior are destructive. A solution could be provided by the application of X-ray µ-CT which was already used in some studies [39,95,96]. This technique will be discussed in detail (comp. 5.3). For a more detailed description of the influencing factors on crack geometry, roughness and tortuosity reference is set to *Mengel et al.* [59].

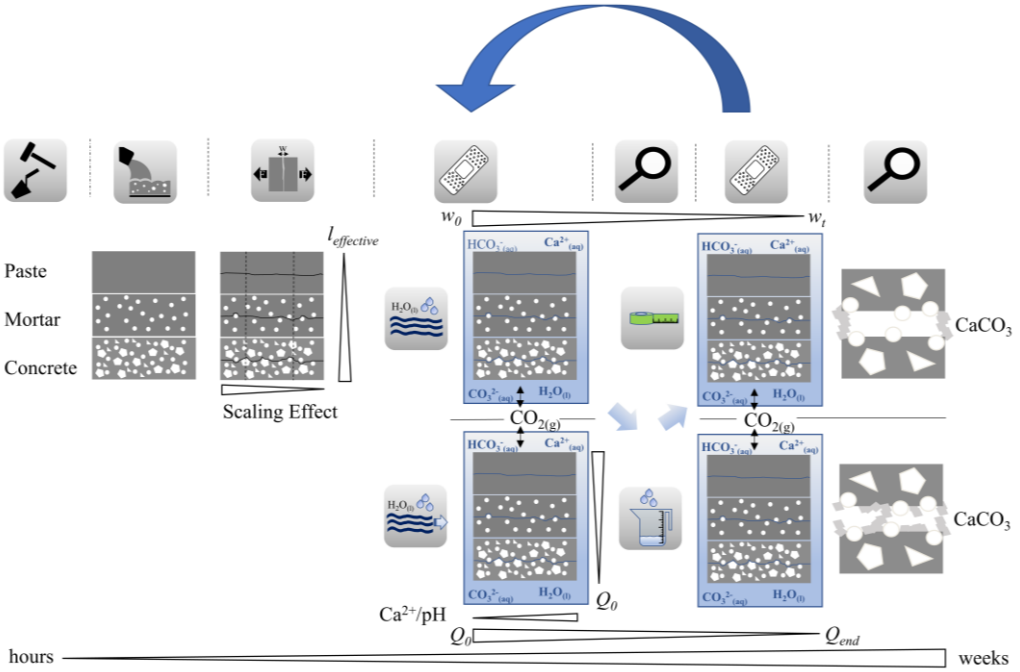

Figure 5. Schematic illustration of the workflow of freshwater immersion and permeability experiments, used materials, cracking, the initiation of healing, monitoring of the healing rate and characterization of healing products, effective crack length ($l_{effective}$), initial crack width (w_0), crack width after a healing period of length t (w_t), initial volume flow (Q_0), volume flow after termination of a self-healing experiment (Q_{end}).

4.4 Exposure to Humidity

Roig-Flores et al. [22] exposed concrete samples to different degrees of relative humidity (**RH**). Specimens subjected to 95 % RH showed a decrease of w by 8 % whereas at 40 % RH w increased by up to 46 %. In both cases neither continued hydration nor calcite precipitation was proven. Respectively, at high RH swelling of the concrete occurred whereas the samples shrunk due to drying at low RH (comp. 2.1). Other studies confirm that continued hydration and calcite precipitation do not occur in humid environments [17,18,37,60,72]. However, it must be addressed that concrete incorporating super-adsorbent polymers (**SAP**) shows the ability of continued hydration and calcite precipitation in humid environments. A detailed discussion is out of the scope of this study. Reference is set to *Snoeck et al.* and *Gruyaert et al.* [53,60,70].

4.5 Exposure to Seawater

Some studies [20,30,31,69] investigated the influence of seawater on autogenous self-healing. Especially in marine environments crack healing is of great importance, since cracks > 10 µm [20,97] can lead to an increased chloride ingress and thus an accelerated deterioration of the reinforcement. Moreover, permeating seawater can impair the functionality of tunnel elements or other concrete structures that must be watertight. The most abundant ions in seawater are Cl^-, Na^+, SO_4^{2-}, Mg^{2+}, Ca^{2+}, K^+ and HCO_3^- in a descending order whereas the concentration of HCO_3^- is roughly the same for seawater and groundwater in equilibrium with the atmosphere. Mg^{2+} shows up to 880 times higher concentrations in seawater than in tap water [98,99].

Therefore, it is not surprising that different chemical causes of autogenous self-healing apply than in freshwater environments. Experimental studies [20,30,31] show that brucite ($Mg(OH)_2$) veined with gypsum ($CaSO_4*2H_2O$), hydrophilite ($CaCl_2$) and ettringite forms directly on the sample surface next to the crack opening when cracked mortar specimens are immersed in artificial seawater for healing. Mg-ions in the water quickly react with hydroxide ions leaching from portlandite and precipitate in form of brucite due to its low solubility. Precipitation of accessory phases such as hydrophilite, gypsum and ettringite is related to the presence of sulphates and sodium chloride in the water. However, the expansive mineral reaction of these phases showed no effect on the rate of self-healing [20]. On top of the brucite layer aragonite deposits which is thermodynamically stabilized by the presence of Mg-ions [47,100–103]. Respectively, the presence of a high Mg^{2+} concentration changes the autogenous self-healing mechanism to the above-mentioned sequence. In contrast, *Danner* et al. [69] found calcite on top of the brucite layer when he investigated concrete beams that were exposed to a marine tidal environment in a Norwegian fjord for 25 years. Thus, the extensive timespan, a cyclic exposure to the atmosphere or other factors imposed by the realistic marine environment may lead to a structural change of aragonite to calcite.

As of today, the influence of different cement types on the extent of autogenous self-healing in marine water is controversial. *Palin et al.* [31] found that autogenous self-healing in artificial seawater is more effective than in fresh water as long as CEM I cement is used. Interestingly, mortar samples based on CEM III show an inverse behavior. This effect was assigned to the lower content of portlandite and lower porosity of CEM III samples and a blocking effect of the brucite layer that might inhibits further leaching of Ca-ions. However, the study lacks chemical prove according to the blocking effect of brucite with respect to the Ca^{2+} diffusion. In

contrast, Dann*er et al.* [69] could not determine any difference in the extend of self-healing for different concrete compositions. According to the experimental setup it must further be addressed that most experiments were carried out on mortar specimens that were immersed in artificial seawater for self-healing. Accordingly, most healing was observed at the crack opening (comp. 4.1, Figure 5) and no mechanical blocking could apply. Only *Palin et al.* [30] tested the water tightness in a permeation experiment. However, the mortar samples were submerged in artificial seawater for 28 and 56 days to initiate self-healing and only subjected to a permeability test of 30 minutes. Thus, the results need to be verified on continuous permeability experiments of cracked concrete. As of today, the scientific knowledge of self-healing of cracked concrete in marine environments is not satisfactory to quantify explicit boundary conditions and transfer results to real concrete structures.

4.6 Conclusion of the causes and Limitations of Autogenous Self-healing

In general, autogenous self-healing is based on the reaction of water and concrete in the restricted space of a separating crack of a certain width. Water, concrete and crack geometry are influenced by various variables that could affect the efficiency of autogenous self-healing. These variables were discussed in the chapters 2, 3 and 4 and are summarized in **Table 5** for the sake of clarity.

Table 5. Effectiveness of experimental variables water, concrete and crack on the efficiency of autogenous self-healing.

Effectiveness	Water	Concrete	Crack
+	• *pH*-value • Temperature • pCO_2 • Water pressure • Water chemistry (c[Mg^{2+}], deionized) • Liquid water	• Aggregate size • Sieve line • Cement content • *W/C* ratio	• Width *w* • Roughness • Tortuosity
-	• Water hardness • Moisture • Sulphates • NaCl	• Aggregate type	
Controversial	• Wet & dry-cycles	• Cement-type • Ca^{2+} availability • Transmission to real concrete structures • Age	• Reinforcement • Fibers
Not investigated	• DOM and other calcite growth inhibiting factors • Real seawater	• Curing Conditions	• Scaling factor (length, depth)

5 Assessment of the Efficiency of Autogenous Self-healing

The extent of autogenous self-healing can be assessed by different approaches such as for instance permeation experiments [10,11,61,64], surface crack width measurements [20,39,49,69], crack width measurements along a cross section [86,91], regain of strength measurements [25,37,60,104] and propagation of ultra-sonic signals [19,29,104,105]. These methods will be discussed in the following paragraphs.

5.1 Recovery of Watertightness

Permeability experiments allow an indirect assessment of the efficiency of autogenous-self-healing by measuring the water flow at certain time Q_t and relating it to the initial water flow Q_0 (**Equation 7**). To determine Q_0 the sample should be water saturated prior to the experiment and time should be given until the flow stabilizes. Accordingly, *Edvardsen* [11] used the average volume flow of the first 5 minutes as Q_0. Generally, experimental setups can be subdivided into two groups [68]: (1) experiments with a constant water head and (2) with a falling water head. Both methods can be used to evaluate self-healing when the test setup is designed according to the theoretical conditions of either Darcy or Poiseuille (comp. 4.3). As previously discussed, autogenous self-healing can also be initiated by water immersion of concrete samples (comp. 4.1). The samples can then be subjected to a permeability test after defined healing periods. Another approach is to initiate healing by the water flow itself inside the permeability test-setup. With the latter a continuous permeation curve can be obtained, and more importantly mechanical blocking and washing out of healing products applies during the whole experiment (comp. 2). The extent of healing S(Q) can be expressed according to (Equation **7**).

$$S_t(Q) = 1 - \frac{Q_t}{Q_0} * 100\% \qquad \textbf{Equation 7}$$

Thus, for a completely healed crack, Q_t is equal to 0 or S is equal to 100 % after a healing period of the length t. However, specimens with a similar crack width can show a severe scatter of volume flow due to variable crack geometries [11,50]. Therefore, it is crucial to assign Q_0 and Q_t to a specific sample and not to a generalized mean surface crack width. Moreover, it is important to list the test duration, volume flow in the beginning and at the end of the experiment. Only then one can estimate whether self-healing is likely in appropriate

time scales and under the given experimental parameters. According to a test series from *Edvardsen*, 5 of 5 samples with a crack width of 100 µm subjected to water flow with a pressure of 0.25 bars healed completely in 28 days. Thus, healing under these experimental conditions is likely to take place although the initial water flow was scattering between 2.92 to 19.25 [$l*(h*m)^{-1}$]. Measuring the permeated water volume indirectly through weight measurements might be the most practicable way. However, it must be addressed that washed out particles can cause a significant error. Therefore, volume flow should also be determined by water level measurements or flow meters. The main advantage of permeation experiments is the water flow itself, which is a crucial factor in water retaining concrete structures. It is also the only method that allows an assessment of the regain of watertightness after a healing period which is an important measure for useability and durability. However, it is not possible to assess the extent and locality of internal healing directly without deterioration of the sample. Thus, water might still be able to reach the rebar and cause corrosion, although a crack exhibits no more water flow. Therefore, permeation experiments should be combined with chemical and mineralogical investigation e.g., of cross sections of the healed crack or the crack surfaces. The pros and cons of this method are summarized in **Table 6**.

Table 6. Overview of the arguments concerning permeability experiments as an evaluation method of the efficiency of autogenous self-healing.

Self-healing Characteristics	Methods	Advantages	Disadvantages
Recovery of watertightness	Permeability test	• Realistic self-healing environment for water retaining concrete structures. • Determination of the water tightness. • Combined healing and monitoring of the extent of self-healing.	• No mineralogical and chemical information of the healing products. • No Information of the locality of crack closing. • Washing out of healing products. • Difficult to apply on large-scale specimens or on construction site. • Complex experimental setup. • No information about the causes and quantity of self-healing. • Sensitive to the measurement conditions but lack of standardized testing.

5.2 Surface Crack Healing

Measurements of the crack closing rate at the surface of a specimen are usually done by either digital or optical (such as polarized-, reflected light-, stereo-microscopy) light microscopic methods but can also be carried out by photography or electron microscopy [39,49,72]. The pros and cons of these methods are summarized in **Table 7**. All approaches have in common that to evaluate crack closing the crack width is determined just before and after a healing period. The extent of healing is then given by the absolute value of the average crack width after the healing

period or expressed as the percentage with respect to the initial width. Alternatively, the crack area A or the pixels of the crack can be determined with image analysis. Generally, it is crucial that the crack width is kept constant during the experiment and the measurements are conducted at the same location. Respectively, setups that use retainers must monitor the relaxation time and the extent of elastic creep before starting any experiment (comp. 3.2). For a regularly monitoring of the healing rate the specimens must be taken out of the healing environment. This can be a source of error in the obtained results. In the literature typically 1, 3, 7, 14, 28 days are used to monitor changes of the self-healing rate in terms of average surface crack width changes [105]. However, surface crack width measurements by nature lack 3D information of the crack closing and as a matter of fact visually healed specimens are not necessarily watertight [70]. Respectively, *Roig-Flores et al.* [22] showed that permeability experiments are the most reliable healing indicators, while crack width measurements show rather good accuracy. Crack area and pixel analysis can show high dispersion. Additionally, polarized, reflected light and electron microscopy can be applied to determine the healing products and the extent of healing [106]. Electron microscopy can provide chemical information by point measurements, profiles or by mapping entire areas. Typically, energy dispersive X-ray spectroscopy (**EDX**) or wavelength dispersive X-ray spectroscopy (**WDX**) allow a chemical characterization, whereas WDX systems have a higher accuracy. With the back scattered electron (**BSE**) mode heavy atoms can be distinguished from light atoms by the signal intensity as the back scattering effect depends on the atomic number. The secondary electron (**SE**) mode allows a detailed view on the surface structure and can be particularly useful to investigate crystal shapes etc. Transmission electron microscopes (**TEM**) further provide the possibility to investigate the crystal structure by electron diffraction, which is similar to X-ray diffraction (**XRD**). However, TEM measurements require thin sections of a few nanometers thickness.

In general, electron microscopic methods measurements are time-consuming and need a destructive sample preparation such as prepared thin sections, a polished surface and/or a gold or carbon sputtering to allow for conductivity. Moreover, special precautions must be taken to avoid hydroxides present in concrete and healing products from evaporation in the low vacuum of the investigation chamber and due to the high energy of the electron beam. Therefore, low vacuum techniques such as the environmental scanning electron microscopy (**ESEM**) are typically used. Concluding, electron microscopical methods provide a powerful tool to investigate the chemical mechanisms and causes of autogenous self-healing within the aforementioned limitations. In contrast, digital-, and stereo-microscopy as well as photography can be carried out without extensive preparation and precautions. Moreover, it is possible to

scan large areas of the sample surface in the lab as well as on site, while crack width is determined in terms of image analysis. As of today, accurate digital hand microscopes are available that are propound for application on construction site and were also applied in a study by *Roig-Flores et al.* [72]. As a concluding remark it must be addressed that to obtain a complete picture of the autogenous self-healing efficiency a combination of methods is recommendable. A comprehensive overview of different methods that can be applied for surface crack width measurement is given by *Ferrara et al.* [107].

Table 7. Overview of the advantages and disadvantages concerning measurements of the surface crack healing as an evaluation method of the efficiency of autogenous self-healing.

Self-healing Characteristics	Methods	Advantages	Disadvantages
Surface crack healing	Digital microscopy*	• Direct determination of the crack width in terms of image analysis. • Spatial information of the crack healing. • No sample preparation. • Can easily be conducted on construction site. • Resolution ~ 1 µm.	• No mineralogical and chemical information of the healing products. • No information about the watertightness. • Experiments must be interrupted to determine self-healing rates.
	Photography*	• See digital microscopy. • Documentation of large areas.	• See digital microscopy.
	Polarized and reflected light microscopy*	• Direct determination of the crack width in terms of image analysis. • Spatial information of the crack healing. • Mineralogical information. • Resolution < 1 µm.	• No chemical information. • Need of destructive sampling and preparation. • Time consuming. • No information about the watertightness.
	Stereo-microscopy*	• See digital microscopy. • Resolution < 1 µm.	• See digital microscopy
	Electron microscopy*	• Direct determination of the crack width in terms of image analysis. • Spatial information of the crack healing. • Resolution ~ 1 nm. • Mineralogical (TEM) and chemical information (EDX, WDX). • Surface structure (SE). • Element distribution (BSE and EDX/WDX mappings).	• Need of destructive sampling and preparation. • No information about the watertightness. • Evaporation of OH-Groups from hydrates due to vacuum and high energy electron beam.

5.3 Internal Crack Healing

Most measurements of the extent of internal crack healing are **destructive** as the sample must be cut or the crack surfaces broken apart to allow an investigation. Therefore, changes of the crack geometry and destruction of a healed intersection might occur. Furthermore, the sample cannot be used for further experiments. As of today, the qualitative assessment of internal crack healing on site is only possible by taking cores (see ultrasound section for a possible future outlook). Measurements are usually done by the same methods applied for surface crack width measurements with the aforementioned pros and cons (comp. 5.2).

A **non-destructive** way to assess the extent of autogenous self-healing is given by **neutron and x-ray radiography and/or tomography** (**Table 8**). See *Snoeck et al.* [105] for a comprehensive overview. Neutron and x-ray radiographic methods were recently applied to investigate the efficiency of intrinsic or engineered healing approaches of cementitious materials [39,49,53,68,95,96,108]. Neutrons interact with the nucleus of the probed matter and are scattered depending on the atomic number of the elements. The scattering probability is higher for nuclei with low atomic numbers such as hydrogen. Therefore, neutron imaging techniques are a perfectly suited tool to assess the water distribution, uptake or permeation in the interior of a sample, while the cement stone and aggregates are almost unaffected by this type of radiation. However, neutron capture can lead to the formation of unstable isotopes that decay and emit radiation. Therefore, specimens subjected to neutron radiation must be checked for radioactivity before further experiments or investigations are carried out. In contrast, x-rays mainly interact with the electrons of an atom, while the attenuation of the radiation increases with increasing atomic number. Concerning the Bouguer-Lambert-Beer equation the attenuation depends on the thickness of the material, the initial intensity of the radiation source and the absorption coefficient of the probed material [109]. Thus, voids, pores and cracks can easily be distinguished from the cement stone and aggregates due to the low absorption coefficient of air. However, the high absorption coefficient of steel, respectively of rebars is problematic as it shields the radiation. Increasing the intensity would lead to an overexposure of the cement stone, aggregates and crack. Therefore, plain concrete specimens should be used in x-ray radiographic investigations. Comparing the attenuation characteristics of neutrons and x-rays it is important to remark that the attenuation coefficients differ due to the different interaction of the radiation with matter. Both have in common that to obtain a 3D model of a specimen through computed tomography (CT), it must be rotated by 360° around a vertical axis during the measurement. The samples should be round in order to avoid edge artifacts [96]. From the different angles cross sections are reconstructed and combined to a 3D model by computational methods [96]. Modern software then allows to extract the crack from the model, calculate the volume or the average width of the crack. However, mayor disadvantages are the high costs of laboratory CTs, long exposure times, the lack of direct mineralogical and chemical information and the restriction to small sample sizes in order to achieve a sufficient resolution for self-healing analysis concerning cracks in the range of 100 to 300 µm. Most common laboratory CTs use divergent radiation beams with the consequence that the resolution decreases with increasing sample size, respectively distance from the radiation source. Therefore, samples are normally only a few cm in height and diameter. An approximation of the resolution of commonly available laboratory

x-ray CTs is given by *Akhavan et al.* [86] with 1/1000 of the sample dimension. Accordingly, the resolution of a 400 mm thick sample is 0.4 mm, which is huge with respect to the crack sizes of interest. However, one solution to the problem could be to fill a crack with epoxy for fixation and then take a core of an area of interest from the sample, which can further be cut to pieces of a few cm in height. Thus, self-healing could take place in samples with realistic dimensions and then be investigated bit by bit through high resolution CT. Finally, it must again be addressed that to obtain a whole picture of the extent of internal self-healing and the corresponding phases and applying chemical processes different methods must be combined.

Ultrasonic testing provides a further non-destructive possibility to obtain information about the extent of internal autogenous self-healing without subjecting small specimens to a time consuming and expansive CT scan (Table 8). Moreover, ultrasound methods are suitable for application on site, generally fast and easy to conduct and can also be applied in a continuous way to monitor changes of the crack interior during self-healing experiments. Commonly applied are impulse based and echo-based techniques. With the latter typically the thickness of concrete components, concrete cover, rebar position etc. are determined. Impulse ultrasound techniques such as ultrasonic pulse velocity (**UPV**), surface transmission, diffuse ultrasound and coda wave interferometry (**CWI**) are suitable to verify the extent of self-healing or the determination of crack depth [105]. In the following focus is laid on UPV. Ultrasound waves are mechanical waves typically in the frequency range of 20 kHz to 10 MHz that are scattered, reflected and partially transmitted at the crack walls of a specimen under investigation. With change of the crack e.g., in depth, width or length the transmitted signal of the elastic wave changes. However, it is important that the crack lays between the transducers in order to record any changes of the signal. For UPV the sensors typically are placed in a straight line on one side or on opposite sides of the sample with the crack laying in-between. At point A the signal is generated and transmitted through the sample. At point B a transducer records the arrival of the wave. Thus, the arrival time, amplitude and attenuation of the waveform in time domain can be recorded. Fast Fourier Transformation (**FFT**) of the time domain allows the transformation to the frequency domain, which can also be useful [105]. Generally, the velocity of ultrasound waves in concrete is approx. 3500 $m*s^{-1}$ and decreases to approx. 343 $m*s^{-1}$ when the wave travels through air, respectively thru a crack [19]. Therefore, the pulse velocity decreases as the ultra-sonic signal crosses a crack. As healing takes place the UPV increases again, while the extent of healing correlates with the regain of pulse velocity [19,29,110,111]. However, Experiments of *Yuan et al.* [19] among others revealed that the initial UPV is not completely restored after a healing experiment which is due to an incomplete and discontinuous

closure of the crack with healing products. To quantify the extent of self-healing with respect to the UPV the healing rate S(UPV) (**Equation 8**) was defined by the latter authors. It includes the UPV V_1 of the cured and uncracked sample, the UPV V_2 of the cracked and the UPV V_3 of the healed sample. A similar approach was proposed by *Tomczak et al.* [110].

$$S(UPV) = \left(1 - \frac{V_1 - V_3}{V_1 - V_2}\right) * 100\ \% \qquad \textbf{Equation 8}$$

It is important to address that ultra-sonic velocity variation in concrete can have various reasons such as pores, cracks, crack geometry and size as well as composition, temperature, humidity and curing conditions [105,110,112]. Therefore, the exact UPV signal is specimen specific and should be measured before crack initiation to allow an assessment of the extent of self-healing. This might be an obstacle for applying the method on construction sites. Moreover, the testing conditions such as the used sensors, cables, sensor position etc. impact the obtained data and should be held constant during a test series. It is also crucial to keep the wavelength of the ultrasound wave bigger than the diameter of the coarsest aggregates to avoid scattering and dissipation of the signal, which is achieved through frequency adjustment [105]. Unfortunately, as of today there is no standardization of the UPV method which makes it difficult to compare data of different publications. Similarly, to the aforementioned UPV measurements waveform and frequency analysis can be applied [19]. The ultrasound signal recorded at point B shows a rapid increase of the amplitude a few µs after a wave impulse is emitted at point A. Then the signal oscillates around the passive state and is attenuated over time by energy conversion. For cracked samples the amplitude is much smaller, while self-healing leads to a restoration of the amplitude. Applying FFT the ultra-sonic signal over time can be transformed to a frequency domain. For uncracked samples the FFT signal shows the highest peak at the excitation frequency of the ultra-sonic source. For cracked specimens the amplitude decreases, and the signal exhibits a shape that is comparable to a noise signal. However, as self-healing takes place the excitation frequency becomes visible in the signal again, while the amplitude correlates with the extent of healing. For both waveform and frequency analysis a self-healing ratio can be formulated as done for the UPV by using the maximum amplitude of the signal or the maximum amplitude of the excitation frequency. All ultra-sonic methods have in common that the extent of self-healing is approximated by restoration of the original signal. However, it is not possible to evaluate the watertightness, the chemical and mineralogical composition of self-healing products or the exact crack width closing the internal healing. Therefore, a combination of methods should be applied. A comprehensive overview of ultrasound testing is given by *Snoeck et al.* [105]. Finally, it must again be addressed that to obtain a whole picture of the efficiency of

autogenous self-healing, the corresponding phases, and applying chemical processes different analytical methods must be combined.

Table 8. Overview of the advantages and disadvantages concerning measurements of the internal crack healing as an evaluation method of the efficiency of autogenous self-healing.

Self-healing Characteristics	Methods	Advantages	Disadvantages
Internal crack healing	*Table 7	• *See surface crack healing.	• *See surface crack healing.
	X-ray CT	• Non-destructive. • 3D model of the crack geometry. • Favorable low X-ray attenuation of air/crack/pores/voids.	• Expansive and time-consuming. • Small samples to obtain a reasonable resolution. • Restricted to the lab. • No chemical and mineralogical information of healing products. • No information about the causes of self-healing. • No information about the watertightness. • Rebar shields the signal. • Round specimens to avoid edge artifacts.
	Neutron CT	• Non-destructive. • 3D model of the specimen. • Determination of the watertightness. Determination of the water distribution.	• Expansive and time-consuming. • Small samples in order to obtain a reasonable resolution. • Restricted to the lab. • No chemical and mineralogical Information of healing products. • No information about the causes of self-healing. • Concrete is almost “invisible”. • Round specimens to avoid edge artifacts. • Not broadly available. • Neutron-capture → radioactivity.
	Ultra-sonic Testing	• Non-destructive. • Assessment of the healing extent. • Assessment of crack depth. • Continuous monitoring is possible. • Practicability. • Can be applied on construction site.	• No chemical and mineralogical information of healing products. • No information about the causes of self-healing. • No information about the exact crack width reduction. • No information about the watertightness. • Sensitive to the measurement conditions but lack of standardized testing.

5.4 Regain of Strength

Regain of strength measurements aim at an indirect assessment of the extent of autogenous self-healing after a specimen was subjected to a healing period. The idea is that strength is reduced due to cracking and restored with healing, whereas the extent of healing is supposed to correlate with the extent of healing or crack closure. However, measurements were found to be independent from calcite precipitation and mainly influenced by the formation of CSH phases [33,34,37,104]. Results of Suleiman et al. [113] agree with these findings and show that the regain of strength is most pronounced for samples incorporating fly ash due to the ongoing pozzolanic reaction. A similar behavior of latent hydraulic cements is expected by the latter authors. In addition, cracked concrete specimens that heal under seawater exposure can show a further decrease in strength due to the cation exchange of Ca^{2+} with Mg^{2+} in CSH phases and the formation of magnesium-silicate-hydrate (MSH) [30,31,114]. Thus, regain of strength

measurements depend on the healing conditions, the cement type and might only be applicable for microcracks or compressed cracks healed by continued hydration (comp. 2.2). Further disadvantages lay in the lack of mineralogical and chemical information as well as the locality of crack healing and the complete deterioration of the sample. It can be concluded that regain of strength measurements are not applicable for evaluating autogenous self-healing of through cracked concrete restricted by Eurocode 1992-3 [14]. The pros and cons of this method are summarized in **Table 9**.

Table 9. Overview of the advantages and disadvantages concerning regain of strength measurements as an evaluation method of the efficiency of autogenous self-healing.

Self-healing Characteristics	Methods	Advantages	Disadvantages
Regain of strength	Compression /Bending /etc.	• Information about the mechanical properties of healed samples.	• Destructive. • Depends on the composition and healing conditions. • No chemical or mineralogical information. • No information about the watertightness. • Self-healing rates cannot be determined.

5.4 Mineralogical and Chemical Assessment of Autogenous Self-healing

Many studies lack comprehensive chemical and mineralogical investigations. Sometimes it can even be observed that certain healing causes are assumed without showing mineralogical or chemical evidence. However, it is desirable that healing phases are qualitatively determined and quantified concerning a comprehensive understanding of the autogenous self-healing process and applying mechanisms. Only then the impact of variables such as the water or concrete composition can be clarified in detail. Generally, raw materials and unaffected reference concrete specimens should be investigated as well as samples subjected to a healing period to allow for a comparison of microstructural and chemical changes [68]. Commonly applied investigation methods are among others microscopy, XRD, electron microscopy, RAMAN spectrometry, Fourier-transform infrared spectroscopy (FTIR), TG/DTA. A detailed discussion of the methods is out of the scope of this study. Reference is set to *Ferrara et al.* [68] and *Snoeck et al.* [105].

6 Conclusion

Based on the findings of this study, the following conclusions can be drawn:

1. Knowledge about the processes and influencing factors of autogenous self-healing is insufficient. Little is known about the quantity of the isolated healing causes and the interlinking of chemical processes as a function of composition and time.

2. The lack of standardized testing makes it difficult to compare literature data. Improvements are proposed at several points within this study. For instance, special care should be taken to conserve the crack geometry when permeability experiments are planned.
3. It was observed that experimental concepts often not cover requirements for the transfer of laboratory results to real concrete structures. Therefore:
    i. Concrete specimens should be used with constant composition within one test series.
    ii. Specimen size should be adapted to real structural component thickness.
    iii. Several specimens should be testes under constant conditions for statistical relevance.
    iv. Crack initiation should be according to the mechanism of load-independent early cracking.
    v. Continuous permeation experiments should be carried out in order to simulate realistic healing conditions of cracked water retaining concrete constructions.
4. A combination of assessment methods should be applied to obtain reliable information on the healing efficiency. Accordingly, watertightness can only be assessed by permeation experiments. For spatial healing information, superficial and internal crack healing must be investigated. To further include the healing causes and processes a comprehensive chemical and mineralogical analysis must be carried out.

Data Availability Statement

Data sharing not applicable to this article as no datasets were generated or analyzed during the current study.

Acknowledgements

This study was funded by the internal research funding of the Helmut-Schmidt-University/University of the Federal Armed Forces Hamburg.

Conflict of Interest

The authors have no conflict of interest relevant for this article.

Received: ((will be filled in by the editorial staff))
Revised: ((will be filled in by the editorial staff))
Published online: ((will be filled in by the editorial staff))

Table 10. Experimental designs and parameters of selected experimental studies investigating self-healing of cracked concrete, sample size (cylindrical specimens: diameter *D* x [height], prismatic specimens: [depth] x [width] x [height])

Authors	Exp. Approach	Pressure [bar]	Number of specimens	Cement type	Cement content [kg*m^{-3}]	Sample type	Sample size	Cracking age [days]	Crack width [µm]	Crack initiation	Start of *Q* [days]	Test duration
[63]	Darcy	0.03	1 per *w*	N/A	344	concrete	D100 mm x 25 mm	90-100	25, 50, 80, 110, 140, 180, 350, 550	TST + LVDT	90-100	20 to 50 days
[67]	Darcy	0.03	2 per *w*	N/A	82 - 115	paste, mortar, concrete	D100 mm x 25/50 mm	28	0, 50, 100, 140, 170, 200, 250, 300, 350	TST + LVDT	28	90 to 100 days
[74]	Darcy	0.03	Total of 12	N/A	82	concrete	D100 mm x 50 mm	29	14 to 350	TST + LVDT	29	90 to 100 days
[29]	Darcy	0.03	3 to 4 per *w*	CEM I 52.5N	300	concrete	D80 mm x 20 mm	365	50 to 870	TST + LVDT	~365	~10 days
[25]	Darcy	0.03	Min. 3 per composition	CEM I 52.5N, CEM II/B-M 32.5N, CEM III/B 32.5	450	mortar	D76 mm x 20mm	55	50 to 350	TST + LVDT	55	28 days
[65]	Darcy	0.01 to 0.09	1 per *w*	N/A	N/A	concrete	D100 mm x 50 mm	N/A	90, 160, 270, 340, 450	TST + LVDT	N/A	N/A
[30]	*Q* [cm^3*s^{-1}]	0.1	10 per *w*	CEM III/B 42.5N-LH	494	mortar	D33.5 mm x 60 mm	28	~200 and ~400	TST + LVDT	28	5,10 und 30 minutes (after 28- and 56-days water immersion)
[22]	*Q* [ml*5min^{-1}]	2 ± 0.05	6 per test series	CEM II/A-L 42.5R	300	concrete	D150 mm x 150 mm	2	< 300	TST + LVDT	3	5 minutes (after 0- and 42-days water immersion)
[53]	Water Column-height (time)	0.002	3 per test series	CEM I 52.5N	510	mortar + SAP	D10 mm x 20 mm	7	~ 200	TST + LVDT	7	Max. 480s
[61]	Poiseuille	N/A	Total of 4, 1 per textile type	CEM III/B 32.5N-NW/HS/NA	550	textile concrete	300 x 100 x 14 mm³	> 7	13 to 65	In-situ tensile test	> 56	21-35 days
[49]	Water Ingress	N/A	3 beams with multiple cracks	CEM I 52.5N	300	concrete	150 x 250 x 3000 mm^3	N/A	100 to 250	PBT	N/A	N/A (after 0 and 49 days)
[70]	*Q* [g*min^{-1}]	0.05, 1 and 2	3 to 5 per composition	CEM I 42.5N	450	mortar + SAP	40 x 40 x 160 mm³	28	130 to 170 → ~ 150	PBT	28	10 minutes
[50]	Poiseuille	0.05	4 to 6 per test series	CEM I 42.5N	450	mortar	40 x 40 x 160 mm^3	7, 14, 28, or 64	150 to 300	PBT	7, 14, 28, or 64	> 5 minutes
[11]	Poiseuille	0.25, 0.5, 1 and 1.5	5 to 11 per test series	CEM lll/A 32.5N, CEM lll/A 32.5N LH/SR, CEM l 32.5R	270 - 300	concrete	200 x 200 x 400 mm³	2	100, 200, 300	Direct tensile test + retainers	28	Up to several weeks

References

[1] F. B. Silva, N. Boon, N. De Belie, W. Verstraete, *J. Commer. Biotechnol.* **2015**, *21*, 31.

[2] S. Yang, F. Aldakheel, A. Caggiano, P. Wriggers, E. Koenders, *Materials (Basel).* **2020**, *13*, 5265.

[3] J. Stark, B. Wicht, *Durability of Concrete*, Springer, Berlin Heidelberg, **2013**.

[4] H. S. Müller, U. Wiens, *Concrete*, John Wiley & Sons, Ltd, **2018**.

[5] H. F. W. Taylor, *Cement Chemistry*, Academic Press, Ltd, London, **1990**.

[6] B. Van Belleghem, S. Kessler, P. Van den Heede, K. Van Tittelboom, N. De Belie, *Cem. Concr. Res.* **2018**, *113*, 130.

[7] N. De Belie, B. Van Belleghem, S. Kessler, P. Van den Heede, K. Van Tittelboom, "Durability Based Service Life Estimation for Chloride Exposed Cracked and Self-Healed Concrete," DOI 10.23967/dbmc.2020.042can be found under https://www.scipedia.com/public/Belie_et_al_2020a, **2020**.

[8] M. de Rooij, K. van Tittelboom, N. De Belie, E. Schlangen, *Self-Healing Phenomena in Cement-Based Materials: State-of-the-Art Report of RILEM Technical Committee*, **2013**.

[9] C. A. Clear, *Cem. Concr. Assoc. Tech. Rep.* **1985**, *559*.

[10] H. Meichsner, *Beton- und Stahlbetonbau* **1992**, *87*, 95.

[11] C. Edvardsen, (PhD Thesis) Water Permeability and Autogenous Healing of Cracks in Concrete, RWTH Aachen, **1996**.

[12] J.-D. Wörner, M. Tsukamoto, *Beton- und Stahlbetonbau* **1993**, *88*, 68.

[13] H. Trost, H. Cordes, B. Ripphausen, *Beton- und Stahlbetonbau* **1989**, *84*, 60.

[14] DIN-EN: 1992-3, *Silos and Tank Structures Made of Concrete*, Germany/Europe, **2011**.

[15] H. Meichsner, S. Röhling, *Der Bausachverständige* **2015**, *11*, 9.

[16] H. Meichsner, S. Röhling, *Beton- und Stahlbetonbau* **2018**, *113*, 307.

[17] N. De Belie, E. Gruyaert, A. Al-Tabbaa, P. Antonaci, C. Baera, D. Bajare, A. Darquennes, R. Davies, L. Ferrara, T. Jefferson, C. Litina, B. Miljevic, A. Otlewska, J. Ranogajec, M. Roig-Flores, K. Paine, P. Lukowski, P. Serna, J. M. Tulliani, S. Vucetic, J. Wang, H. M. Jonkers, *Adv. Mater. Interfaces* **2018**, *5*, 1800074.

[18] A. R. Suleiman, M. L. Nehdi, *Cem. Concr. Res.* **2018**, *111*, 197.

[19] L. Yuan, S. Chen, S. Wang, Y. Huang, Q. Yang, S. Liu, J. Wang, P. Du, X. Cheng, Z. Zhou, *Materials (Basel).* **2019**, *12*, 2818.

[20] M. Maes, (PhD Thesis) Combined Effects of Chlorides and Sulphates on Cracked and Self-Healing Concrete in Marine Environments, Ghent University, **2015**.

[21] K. Van Tittelboom, N. De Belie, *Materials (Basel).* **2013**, *6*, 2182.

[22] M. Roig-Flores, S. Moscato, P. Serna, L. Ferrara, *Constr. Build. Mater.* **2015**, *86*, 1.

[23] H. Ritzmann, *Zement-Kalk-Gips* **1968**, *21*, 390.

[24] K. Krenkler, *Chemie Des Bauwesens Band 1: Anorganische Chemie*, Springer, Berlin Heidelberg New York, **1980**.

[25] K. Van Tittelboom, E. Gruyaert, H. Rahier, N. De Belie, *Constr. Build. Mater.* **2012**, *37*, 349.

[26] H. Huang, (PhD Thesis) Thermodynamics of Autogenous Self-Healing in Cementitious Materials, Technische Universiteit Delft, **2015**.

[27] H. Huang, G. Ye, D. Damidot, *Cem. Concr. Res.* **2013**, *52*, 71.

[28] H. Rahmani, H. Bazrgar, *Mag. Concr. Res.* **2015**, *67*, 476.

[29] K. Van Tittelboom, N. De Belie, W. De Muynck, W. Verstraete, *Cem. Concr. Res.* **2010**, *40*, 157.

[30] D. Palin, H. M. Jonkers, V. Wiktor, *Cem. Concr. Res.* **2016**, *84*, 1.

[31] D. Palin, V. Wiktor, H. M. Jonkers, *Cem. Concr. Res.* **2015**, *73*, 17.

[32] M. Şahmaran, H. A. Christianto, I. Ö. Yaman, *Cem. Concr. Compos.* **2006**, *28*, 432.

[33] P. Termkhajornkit, T. Nawa, Y. Yamashiro, T. Saito, *Cem. Concr. Compos.* **2009**, *31*, 195.

[34] Z. Zhou, Z. Li, D. Xu, J. Yu, *Adv. Mater. Res.* **2011**, *306–307*, 1020.

[35] M. Şahmaran, V. C. Li, *Cem. Concr. Res.* **2009**, *39*, 1033.

[36] X. Liu, W. Yao, X. Zheng, J. WU, *J. Build. Mater.* **2005**, *2*, 184.

[37] N. ter Heide, E. Schlangen, in *Proc. First Int. Conf. Self Heal. Mater. Noordwijk Aan Zee, 18-20 April*, **2007**.

[38] D. Snoeck, (PhD Thesis) Self-Healing and Microstructure of Cementitious Materials with Microfibres and Superabsorbent Polymers, Ghent University, **2015**.

[39] A. R. Suleiman, A. J. Nelson, M. L. Nehdi, *Cem. Concr. Compos.* **2019**, *103*, 49.

[40] DAfStb, *Erläuterungen Zu Den Normen DIN EN 206-1, DIN 1045-2, DIN 1045-3, DIN 1045-4 Und DIN EN 12620 - DAfStb-Heft 526*, Beuth Verlag, Berlin, **2011**.

[41] M. M. Reddy, G. H. Nancollas, *J. Colloid Interface Sci.* **1971**, *36*, 166.

[42] G. H. Nancollas, M. M. Reddy, *J. Colloid Interface Sci.* **1971**, *37*, 824.

[43] E. Ruiz-Agudo, C. V. Putnis, C. Rodriguez-Navarro, A. Putnis, *Geochim. Cosmochim. Acta* **2011**, *75*, 284.

[44] B. Kunz, (PhD Thesis) Heterogene Nukleierun Und Kristallwachstum van CaCO3 (Calcit) in Natürlichen Gewässern, ETH Zürich, **1983**.

[45] K. E. Chave, E. Suess, *Limnol. Oceanogr.* **1970**, *15*, 633.

[46] K. Simkiss, *Biol. Rev.* **1964**, *39*, 487.

[47] M. R. Nielsen, K. K. Sand, J. D. Rodriguez-Blanco, N. Bovet, J. Generosi, K. N. Dalby, S. L. S. Stipp, *Cryst. Growth Des.* **2016**, *16*, 6199.

[48] DAfStb, *Wasserundurchlässige Bauwerke Aus Beton (WU-Richtlinie)*, Beuth Verlag, Berlin, **2017**.

[49] K. Van Tittelboom, J. Wang, M. Araújo, D. Snoeck, E. Gruyaert, B. Debbaut, H. Derluyn, V. Cnudde, E. Tsangouri, D. Van Hemelrijck, N. De Belie, *Constr. Build. Mater.* **2016**, *107*, 125.

[50] T. Van Mullem, E. Gruyaert, B. Debbaut, R. Caspeele, N. De Belie, *Constr. Build. Mater.* **2019**, *203*, 541.

[51] DIN-EN: 206-1, *Concrete - Specification Properties, Production and Conformity*, **2017**.

[52] S. Ahmad, A. K. Azad, K. F. Loughlin, *J. Adv. Concr. Technol.* **2012**, *10*, 86.

[53] D. Snoeck, S. Steuperaert, K. Van Tittelboom, P. Dubruel, N. De Belie, *Cem. Concr. Res.* **2012**, *42*, 1113.

[54] R. K. Dhir, C. M. Sangha, J. G. L. Munday, *J Am Concr. Inst* **1973**, *70*, 231.

[55] D. J. Hannant, J. G. Keer, *Cem. Concr. Res.* **1983**, *13*, 357.

[56] K. R. Lauer, F. O. Slate, *Mater. Construcción* **1957**, *7*, 51.

[57] P. M. B. R. K. Nanduri, *Int. J. Civ. Eng. Technol.* **2021**, *11*, 74.

[58] W. Henning, (PhD Thesis) Zwangrissbildung Und Bewehrung von Stahlbetonwänden Auf Steifen Unterbauten, Technische Universität Braunschweig, **1987**.

[59] L. Mengel, H. W. Krauss, D. Lowke, *Constr. Build. Mater.* **2020**, *254*, 118990.

[60] D. Snoeck, N. De Belie, *J. Mater. Civ. Eng.* **2016**, *28*, 4015086.

[61] V. Mechtcherine, M. Lieboldt, *Cem. Concr. Compos.* **2011**, *33*, 725.

[62] C.-M. Aldea, S. P. Shah, A. Karr, *Mater. Struct.* **1999**, *32*, 370.

[63] K. Wang, D. C. Jansen, S. P. Shah, A. F. Karr, *Cem. Concr. Res.* **1997**, *27*, 381.

[64] H. W. Reinhardt, M. Jooss, *Cem. Concr. Res.* **2003**, *33*, 981.

[65] K. J. Shin, W. Bae, S. W. Choi, M. W. Son, K. M. Lee, *Constr. Build. Mater.* **2017**, *151*, 907.

[66] L. Japaridze, *J. Rock Mech. Geotech. Eng.* **2015**, *7*, 509.

[67] C.-M. Aldea, S. P. Shah, A. Karr, *J. Mater. Civ. Eng.* **1999**, *11*, 181.

[68] L. Ferrara, T. Van Mullem, M. C. Alonso, P. Antonaci, R. P. Borg, E. Cuenca, A. Jefferson, P. L. Ng, A. Peled, M. Roig-Flores, M. Sanchez, C. Schroefl, P. Serna, D. Snoeck, J. M. Tulliani, N. De Belie, *Constr. Build. Mater.* **2018**, *167*, 115.

[69] T. Danner, U. H. Jakobsen, M. R. Geiker, *Minerals* **2019**, *9*, 284.

[70] E. Gruyaert, B. Debbaut, D. Snoeck, P. Díaz, A. Arizo, E. Tziviloglou, E. Schlangen, N. De Belie, *Smart Mater. Struct.* **2016**, *25*, 084007.

[71] T. Van Mullem, G. Anglani, M. Dudek, H. Vanoutrive, G. Bumanis, C. Litina, A. Kwiecień, A. Al-Tabbaa, D. Bajare, T. Stryszewska, R. Caspeele, K. Van Tittelboom, T. Jean-Marc, E. Gruyaert, P. Antonaci, N. De Belie, *Sci. Technol. Adv. Mater.* **2020**, *21*, 661.

[72] M. Roig-Flores, P. Serna, *Sustain.* **2020**, *12*, 4476.

[73] H. Liu, H. Huang, X. Wu, H. Peng, Z. Li, J. Hu, Q. Yu, *Cem. Concr. Res.* **2019**, *120*, 198.

[74] C.-M. Aldea, W.-J. Song, J. S. Popovics, S. P. Shah, *J. Mater. Civ. Eng.* **2000**, *12*, 92.

[75] W. Wittke, *Rock Mechanics*, Springer, Berlin Heidelberg, **1984**.

[76] B. Hölting, W. G. Coldewey, *Hydrogeology*, Springer Spektrum, Berlin Heidelberg, **2013**.

[77] N. Hearn, *Mater. Struct. Constr.* **1998**, *31*, 563.

[78] N. Hearn, R. J. Detwiler, C. Sframeli, *Cem. Concr. Res.* **1994**, *24*, 633.

[79] T. C. Powers, *Chem. Cem. Proc. Fourth Int. Symp.* **1960**, *2*, 577.

[80] T. C. Powers, J. C. Copeland, H. M. Mann, *Portl. Cem. Assoc.* **1959**, *1*, 38.

[81] M. R. Nokken, R. D. Hooten, in *1st Int. RILEM Symp. Adv. Concr. Through Sci. Eng. Evanst. Illinois, 21-24 March*, RILEM Publications SARL, **2004**.

[82] K. Wu, L. Xu, G. De Schutter, H. Shi, G. Ye, *J. Adv. Concr. Technol.* **2015**, *13*, 169.

[83] K. Wu, (PhD Thesis) Experimental Study on the Influence of ITZ on the Durability of Concrete Made with Different Kinds of Blended Materials, Ghent University, **2014**.

[84] C. Louis, (PhD Thesis) Strömungsvorgänge in Klüftigen Medien Und Ihre Wirkung Auf Die Standsicherheit von Bauwerken Und Böschungen Im Fels, TH Karlsruhe, **1967**.

[85] G. Rastiello, C. Boulay, S. Dal Pont, J. L. Tailhan, P. Rossi, *Cem. Concr. Res.* **2014**, *56*, 20.

[86] A. Akhavan, S. M. H. Shafaatian, F. Rajabipour, *Cem. Concr. Res.* **2012**, *42*, 313.

[87] H. Meichsner, *Beton- und Stahlbetonbau* **1992**, *87*, 299.

[88] F. M. White, *Viscous Fluid Flow*, McGraw-Hill, Inc., New York, **1991**.

[89] G. M. Lomize, *Water Flow Through Jointed Rock (Russian)*, Gosenergoizdat, **1951**.

[90] P. Rißler, (PhD Thesis) Bestimmung Der Wasserdurchlässigkeit von Kluftigem Fels, RWTH Aachen, **1977**.

[91] P. J. Yannopoulos, *Mag. Concr. Res.* **1989**, *41*, 63.

[92] A. W. Beeby, R. H. Scott, *Mag. Concr. Res.* **2005**, *57*, 611.

[93] S. Husain, P. Ferguson, *Flexural Crack Width at the Bars in Reinforced Concrete*, Research Report 102-IF, **1968**.

[94] B. Brooms, *Am. Concr. Inst. J.* **1965**, 1237.

[95] D. Fukuda, Y. Nara, Y. Kobayashi, M. Maruyama, M. Koketsu, D. Hayashi, H. Ogawa, K. Kaneko, *Cem. Concr. Res.* **2012**, *42*, 1494.

[96] S. Brisard, M. Serdar, P. J. M. Monteiro, *Cem. Concr. Res.* **2020**, *128*, 105824.

[97] I.-S. Yoon, E. Schlangen, *KSCE J. Civ. Eng.* **2014**, *18*, 188.

[98] Hamburg Wasser, "Tap water from Glinde," can be found under https://www.hamburgwasser.de/fileadmin/hhw-privatkunden/downloads/wasseranalysen/hamburgwasser-unser-wasser-wasseranalyse-glinde.pdf, accessed: 06.04.2022, **2020**.

[99] LENNTECH, "Major ion composition of seawater (mg/L)," can be found under https://www.lenntech.com/composition-seawater.htm, accessed: 06.04.2022, **2005**.

[100] R. A. Berner, J. W. Morse, *Am. J. Sci.* **1974**, *274*, 108.

[101] R. A. Berner, *Geochim. Cosmochim. Acta* **1975**, *39*, 495.

[102] K. J. Davis, P. M. Dove, J. J. De Yoreo, *Science (80-.).* **2000**, *290*, 1134.

[103] Y. Zhang, R. A. Dawe, *Chem. Geol.* **2000**, *163*, 129.

[104] S. Jacobsen, E. J. Sellevold, *Cem. Concr. Res.* **1996**, *26*, 55.

[105] D. Snoeck, F. Malm, V. Cnudde, C. U. Grosse, K. Van Tittelboom, *Adv. Mater. Interfaces* **2018**, *5*, 1800179.

[106] A. Putnis, *Introduction to Mineral Sciences*, Cambridge University Press, Cambridge New York Port Chester Melbourne Sydney, **1992**.

[107] L. Ferrara, E. C. Asensio, F. Lo Monte, M. R. Flores, M. S. Moreno, D. Snoeck, T. Van Mullem, N. De Belie, in *18th Int. Conf. Exp. Mech. (ICEM 2018), Brussels (Belgium), 1-5 July*, **2018**.

[108] F. A. Gilabert, K. Van Tittelboom, J. Van Stappen, V. Cnudde, N. De Belie, W. Van Paepegem, *Cem. Concr. Compos.* **2017**, *77*, 68.

[109] T. G. Mayerhöfer, S. Pahlow, J. Popp, *ChemPhysChem* **2020**, *21*, 2029.

[110] K. Tomczak, J. Jakubowski, Ł. Kotwica, *Materials (Basel).* **2020**, *13*, 3336.

[111] G. Lefever, D. Snoeck, N. De Belie, S. Van Vlierberghe, D. Van Hemelrijck, D. G. Aggelis, *Sensors (Switzerland)* **2020**, *20*, 2959.

[112] H. Güneyli, S. Karahan, A. Güneyli, N. Yapıcı, *Russ. J. Nondestruct. Test.* **2017**, *53*, 159.

[113] A. R. Suleiman, M. L. Nehdi, *Sci. Rep.* **2021**, *11*, 7245.

[114] D. Bonen, *J. Am. Ceram. Soc.* **1992**, *75*, 2904.

Daniel Lahmann studied mineralogy at the Georg-August University Göttingen. He graduated with a master´s degree in 2021 and has since been working as a doctoral student in Prof. Kessler's research group at the Institute of Engineering Materials and Building Preservation at the Helmut-Schmidt-University Hamburg. He is currently conducting research on autogenous self-healing of concrete.

Dr. Sylvia Kessler is Full Professor for Engineering Materials and Building Preservation at the Helmut-Schmidt-University / University of the Federal Armed Forces Hamburg. She received her master's degree in civil engineering from RWTH Aachen University and her PhD in civil engineering from the Technical University Munich. She is currently conducting and supervising research on Concrete Durability and Sustainability, Structural Health Monitoring, Non-destructive Testing, Probability-based Service Life Design and Condition Assessment of Reinforced Concrete Structures.

Dr. Carola Edvardsen is a chief concrete specialist at COWI. She graduated in civil engineering and received her PhD from RWTH Aachen University on autogenous self-healing of cracks in concrete. She is currently responsible for COWI´s activities within concrete durability technology and service life design for structures in general, which include bridge, tunnel and marine structures in particular.

Table of contents entry:

Concrete exhibits an intrinsic ability to heal cracks, defined as “autogenous self-healing”. However, despite code restrictions, autogenous self-healing of concrete shows limited effectiveness in practice. This indicates the need for further research to provide engineers with reliable design rules. Therefore, this study aims for giving a broad literature review on the state-of-the-art knowledge on autogenous self-healing, experimental designs and applied test methods.

Daniel Lahmann, Carola Edvardsen and Sylvia Kessler*

Autogenous Self-Healing of Concrete: Experimental Design and Test Methods – A Review